

Coherent Photo- and Leptoproduction of Vector Mesons from Deuterium

L. Frankfurt^{a,e}, W. Koepf^b, J. Mutzbauer^c,
G. Piller^c, M. Sargsian^{c,f}, M. Strikman^{d,e}
(February 12, 2018)

- (a) School of Physics and Astronomy, Tel Aviv University, Tel Aviv, 69978 Israel
- (b) Physics Department, Ohio State University, Columbus, OH 43210, USA
- (c) Physik Department, Technische Universität München, D-85747 Garching, Germany
- (d) Pennsylvania State University, University Park, PA 16802, USA
- (e) Institute for Nuclear Physics, St. Petersburg, Russia
- (f) Yerevan Physics Institute, Yerevan 375036, Armenia

Abstract

We discuss the coherent photo- and leptoproduction of vector mesons from deuterium at intermediate (virtual) photon energies, $3\text{ GeV} \lesssim \nu \lesssim 30\text{ GeV}$. These processes provide several options to explore the space-time evolution of small size quark-gluon configurations. Furthermore, we study the dependence of the production cross section on the energy and momentum transfer t due to variations of the finite longitudinal interaction length. Kinematic regions are determined where the production cross section is most sensitive to the final state interaction of the initially produced hadronic wave packet. For unpolarized deuteron targets this double scattering contribution can be investigated mainly at large values of the momentum transfer t . For polarized targets kinematic windows sensitive to double scattering are available also at moderate t . We suggest several methods for an investigation of color coherence effects at intermediate energies.

I. INTRODUCTION

High-energy exclusive production processes from nucleon targets are determined by the transition of initial partonic wave functions to final hadronic states. Interesting details about the corresponding amplitudes can be obtained by embedding the production process into nuclei, where the formation of a particular hadron is probed via the interaction with spectator nucleons (for recent reviews see e.g. [1]).

In this context we discuss the coherent photo- and leptonproduction of vector mesons from unpolarized as well as polarized deuterium at photon energies $\nu \gtrsim 3 \text{ GeV}$ ($q^\mu = (\nu, \mathbf{q})$ is the photon four-momentum and $Q^2 = -q^2$):

$$\gamma^{(*)} + \overset{(\rightarrow)}{d} \longrightarrow V + d. \quad (1)$$

The corresponding amplitudes can be split into two pieces: a single scattering term in which only one nucleon participates in the interaction, and a double scattering contribution. In this double scattering term the (virtual) photon interacts with one of the nucleons inside the target and produces an intermediate hadronic state which subsequently re-scatters from the second nucleon before forming the final state vector meson.

At small $Q^2 \lesssim 1 \text{ GeV}^2$ and intermediate energies, $3 \text{ GeV} \lesssim \nu \lesssim 30 \text{ GeV}$, exclusive vector meson production from deuterium is well understood in terms of vector meson dominance. Here, as seen from the laboratory frame, the final state vector meson is formed prior to the interaction with the target (for a summary and references see e.g. [2]). On the other hand in the limit of large $Q^2 \gg 1 \text{ GeV}^2$ perturbative QCD calculations show that photon-nucleon scattering produces a small-sized color singlet quark-gluon wave packet (ejectile) instead of a soft vector meson [3].¹ At large energies ν the re-scattering of such an ejectile with the second nucleon should differ substantially from the re-scattering of a soft vector meson. Therefore the magnitude of the double scattering contribution to the production process contains interesting informations about the initially produced ejectile and its evolution while propagating through the target.

The ejectile wave packet and its propagation are characterized by the following scales: the average **transverse size** of the wave packet which for the case of longitudinal photons is $b_{ej} \approx 4 \dots 5/Q$ for the contribution of the minimal Fock space component at $Q^2 \gtrsim 5 \text{ GeV}^2$ [6]. For these Q^2 it amounts to less than a third of the typical diameter of a ρ -meson ($\approx 1.2 \text{ fm}$). Furthermore, the initially produced small quark-gluon wave packet does not, in general, represent an eigenstate of the strong interaction Hamiltonian. Expanding the ejectile in hadronic eigenstates one finds that inside a nuclear target all hadronic components, except the measured vector meson, are filtered out via final state interaction after a typical **formation time**: $\tau_f \approx 2\nu/\delta m_V^2$. Here δm_V^2 is the characteristic difference of the squared masses of low-lying vector meson states which is related to the inverse slope of the corresponding Regge trajectory ($\delta m_V^2 \sim 1 \text{ GeV}^2$). If the formation time is larger than the nuclear radius the coherence between the hadronic eigenstates, which describe the ejectile, is

¹ Note that this decrease of the “size” of the virtual photon at large Q^2 has been already suggested before the advent of QCD (see e.g. Refs. [2,4,5]).

kept on the scale of the target dimensions. Then the transverse size of the ejectile is frozen during its penetration through the target. Contributions from re-scattering processes should therefore decrease with rising Q^2 at large photon energies. This phenomenon is commonly called color coherence or color transparency [1].

However, it has been understood for more than twenty years that dominant contributions to high-energy, photon-induced processes result from large longitudinal space-time intervals which increase with energy [7–9]. As soon as they are of the order of the average nucleon-nucleon distance in nuclei nuclear effects become important. A well known experimental confirmation of this fact can be found in nuclear deep-inelastic scattering at small values of the Bjorken scaling variable $x = Q^2/2M\nu$, where M is the nucleon mass. Here the increase of the longitudinal interaction distance $\sim 1/2Mx$ (see e.g. [10]) which dominates the reaction at small x leads to the leading twist shadowing of parton distributions in nuclei at $x \ll 0.1$ (for a recent review see Ref. [11]).

For diffractive vector meson production from nuclei the situation is similar. Here the **characteristic longitudinal interaction length**² $\lambda \approx 2\nu/(m_V^2 + Q^2)$ is determined by the minimal momentum transfer, $t_{min} = -1/\lambda^2$, required for the diffractive production of the vector meson with invariant mass m_V . In the kinematic domain of intermediate photon energies $\nu \lesssim 30 \text{ GeV}$ and $Q^2 \gtrsim 1 \text{ GeV}^2$, which is accessible for example at HERMES, λ is of the order of typical nuclear dimensions and can have a major influence on the scattering process. Note that for $Q^2 > 3 \text{ GeV}^2$ the same is true even for large photon energies $\nu \lesssim 150 \text{ GeV}$ as available at FNAL. Therefore if one investigates the double scattering contribution to diffractive vector meson production in different kinematic regions one should be careful in interpreting a variation of the re-scattering strength as a modification of the ejectile wave function. First, possible effects arising from a variation of the characteristic longitudinal interaction length have to be investigated. For total production cross sections and differential cross sections at small momentum transfers, $t \approx 0$, they are accounted for in the framework of the Glauber multiple scattering theory [2,12–14]. However, as we will show, Glauber theory does not reproduce the proper longitudinal interaction length in vector meson production at $t \neq 0$, since it neglects nuclear recoil effects which turn out to be important for light nuclei.

The privileged use of deuterium as a target has several reasons: first the deuteron is the simplest bound state of nucleons and therefore the “best” understood nucleus. Its wave function is known within a few percent accuracy at least up to internal momenta $\lesssim 400 \text{ MeV}/c$, and further insights on the high momentum tail of the deuteron wave function are expected from current experiments at MAMI, NIKHEF and TJNAF. This provides many possibilities to investigate double scattering processes on different characteristic length scales using for example polarized targets or tagging on specific break-up proton-neutron final states.

Note that in inclusive vector meson production from heavy nuclei the formation length is larger than the size of the nuclear target only at large photon energies. This makes an analysis of color coherence effects at moderate energies more difficult. Also many exclusive channels in vector meson production from heavy nuclei suffer from theoretical uncertainties related to the more complicated final state interaction of the detected hadrons.

² A detailed discussion of the t -dependence of λ is presented in Sec.III C.

This paper is organized as follows: in Sec.II we review the derivation of the single and double scattering amplitudes for diffractive vector meson production. The differential production cross section for coherent processes is derived in Sec.III. There, after showing evidence for double scattering events, we discuss effects due to the kinematic dependence of the finite longitudinal interaction length and suggest corresponding experiments feasible at TJNAF and HERMES. We then propose signatures for color coherence at large and moderate momentum transfers suitable for investigations at HERMES. Conclusions follow in Sec.IV

II. PHOTON-DEUTERON SCATTERING AMPLITUDE

In view of the high energy of the incident photon we derive the vector meson production amplitude within the eikonal approximation. This can be done for coherent as well as incoherent diffractive production processes. In the next section we then focus on the coherent case. The following notations are used: $p_d^\mu = (M_d, \mathbf{0})$ is the deuteron four-momentum in the laboratory frame which we will use throughout this investigation. The final state proton-neutron system with invariant mass M_f is either a deuteron or a proton-neutron continuum state (pn). Its four-momentum is denoted by p_f^μ . Furthermore, $q^\mu = (\nu, \mathbf{0}_\perp, \sqrt{Q^2 + \nu^2})$ and k_V are the momenta of the incident photon and the produced vector meson, respectively. They determine the momentum transfer to the deuteron, $l^\mu = (l_0, \mathbf{l}) = q^\mu - k_V^\mu$.

In the impulse approximation the vector meson is produced either from the proton or the neutron. The corresponding diagram is shown in Fig.1a. In a non-relativistic treatment of the deuteron target and the final pn system we obtain for the single scattering amplitude:

$$F^{(a)} = f^{\gamma^* p \rightarrow V p}(\mathbf{l}) S_{df}^{jj'} \left(-\frac{\mathbf{l}_\perp}{2}, \frac{l_-}{2} \right) + f^{\gamma^* n \rightarrow V n}(\mathbf{l}) S_{df}^{jj'} \left(\frac{\mathbf{l}_\perp}{2}, -\frac{l_-}{2} \right). \quad (2)$$

Here only the dependence of the photon-nucleon production amplitudes $f^{\gamma^* N \rightarrow V N}$ on the corresponding three-momentum transfer is shown explicitly. Furthermore we have introduced the non-relativistic transition form factor (the corresponding relativistic expression is given in Appendix A):

$$S_{df}^{jj'}(\mathbf{l}) = \int d^3k \psi_d^j \left(\mathbf{k} + \frac{\mathbf{l}}{2} \right) \psi_f^{j'\dagger} \left(\mathbf{k} - \frac{\mathbf{l}}{2} \right) = \int d^3r \psi_d^j(\mathbf{r}) \psi_f^{j'\dagger}(\mathbf{r}) e^{-i\mathbf{l}\cdot\mathbf{r}}, \quad (3)$$

where ψ_d^j is the wave function of the deuteron target with spin quantum numbers j , and $\psi_f^{j'}$ denotes the wave function of the final pn system with spin j' . Bound state wave functions are normalized according to $\int d^3k |\psi_d(\mathbf{k})|^2 = 1$, while two-nucleon continuum wave functions obey $\int d^3k \psi_f^P(\mathbf{k}) \psi_f^{P'+}(\mathbf{k}) = \delta^3(\mathbf{P} - \mathbf{P}')$, where \mathbf{P} and \mathbf{P}' are the momenta of the pn state with energy $E = \mathbf{P}^2/2M$. Throughout the paper all amplitudes are normalized according to $Im f^{VN \rightarrow VN}(l=0) = \sigma_{VN}$, the latter being the total vector meson-nucleon cross section. Here and in the following we temporarily suppress the spin dependence of the scattering amplitudes. Note that Eq.(2) corresponds to the well known result of Refs. [15,16] except for the presence of $l_- = l_0 - l_z = \sqrt{M_f^2 + \mathbf{l}^2} - M_d - l_z$ in the form factor. The latter accounts for the recoil of the two-nucleon system (see Appendix A).

In the double scattering contribution the vector meson is produced via an intermediate hadronic state h as shown in Fig.1b. The corresponding amplitude reads:

$$F^{(b)} = - \int \frac{d^3 p_s d^3 p'_s}{(2\pi)^3} \psi_d^j(-\mathbf{p}_s) \frac{f^{\gamma^* p \rightarrow hp}(\mathbf{l}_\perp - \mathbf{k}_\perp) k_h^0 f^{hn \rightarrow Vn}(\mathbf{k}_\perp)}{D_h(q - l + k)} \\ \times \psi_f^{j'\dagger} \left(\frac{\mathbf{l}_\perp}{2} - \mathbf{k}_\perp - \mathbf{p}_{s\perp}, -\frac{l_-}{2} + k_- - p_{sz} \right) + (p \leftrightarrow n). \quad (4)$$

where p_s and p'_s are the four-momenta of the spectator nucleon before and after the re-scattering of the intermediate hadronic state h and $k = p'_s - p_s$. Similar to single scattering we account for the recoil of the two-nucleon final state (see Appendix A, Eq.(A6)). Note that in the derivation of Eq.(4) completeness over the two-nucleon intermediate states has been used.

The intermediate state h carries an invariant mass m_h and a four-momentum $k_h = k_V + k = q - l + k$. Its propagator leads to the denominator $D_h(k_h) = k_h^2 - m_h^2 + i\epsilon$. In Eq.(4) we have assumed that the diffractive amplitudes f depend on the corresponding transverse momentum transfer only. This is justified by the fact that momenta characteristic for bound nucleons have negligible effects on the amplitudes f . Consequently the light-cone momentum l_- enters effectively only in the form factor and propagator of the intermediate hadronic state. After introducing $P = (p'_s + p_s)/2$ one can factorize the integrations in (4) and obtains:

$$F^{(b)} = - \int \frac{d^3 k}{(2\pi)^3} S_{df}^{jj'} \left(-\frac{\mathbf{l}_\perp}{2} + \mathbf{k}_\perp, \frac{l_-}{2} - k_- \right) \frac{f^{\gamma^* p \rightarrow hp}(\mathbf{l}_\perp - \mathbf{k}_\perp) k_h^0 f^{hn \rightarrow Vn}(\mathbf{k}_\perp)}{D_h(q - l + k)} + (p \leftrightarrow n). \quad (5)$$

Substituting $-l/2 + k \rightarrow k$ leads to:

$$F^{(b)} = - \int \frac{d^3 k}{(2\pi)^3} S_{df}^{jj'}(\mathbf{k}_\perp, -k_-) \frac{f^{\gamma^* p \rightarrow hp}(\frac{\mathbf{l}_\perp}{2} - \mathbf{k}_\perp) k_h^0 f^{hn \rightarrow Vn}(\frac{\mathbf{l}_\perp}{2} + \mathbf{k}_\perp)}{D_h(q - \frac{l}{2} + k)} + (p \leftrightarrow n). \quad (6)$$

Within the non-relativistic approximation for the initial and final proton-neutron system the denominator of the intermediate hadron can be reduced to:

$$D_h(q - \frac{l}{2} + k) = \left(q - \frac{l}{2} + k \right)^2 - m_h^2 + i\epsilon \\ \approx 2k_h^0 \left[k_- - \frac{l_-}{2} - \frac{(\frac{l}{2} - \mathbf{k})^2}{2\nu} - \frac{Q^2 + m_h^2}{2\nu} + i\epsilon \right], \quad (7)$$

where only leading terms with respect to the photon energy are kept. The denominator in Eq.(7) can be simplified further using the empirical fact that diffractive amplitudes can be parameterized by $f(\mathbf{k}) \sim e^{-\frac{B}{2}\mathbf{k}^2}$, with a typical slope of $B \sim (5 - 8) \text{ GeV}^{-2}$ depending on Q^2 and ν [2,17]. Consequently, at large photon energies we can neglect the term $(\frac{l}{2} - \mathbf{k})^2/2\nu \lesssim 1/B\nu$. Furthermore we omit $k_0 \approx \mathbf{k}_\perp^2/2M$ which is small due to the transition form factor in Eq.(6) which favors contributions from $\mathbf{k}_\perp^2 \approx 0$. Substituting Eq.(7) into Eq.(6) gives:

$$F^{(b)} = - \int \frac{d^3k}{2(2\pi)^3} S_{df}^{jj'}(\mathbf{k}) \frac{f^{\gamma^*p \rightarrow hp}(\frac{\mathbf{l}_\perp}{2} - \mathbf{k}_\perp) f^{hn \rightarrow Vn}(\frac{\mathbf{l}_\perp}{2} + \mathbf{k}_\perp)}{-k_z - \Delta_h + i\epsilon} + (p \leftrightarrow n), \quad (8)$$

$$\text{with } \Delta_h = \frac{l_z}{2} + \frac{Q^2 + m_h^2}{2\nu} = \frac{Q^2 + 2m_h^2 - m_V^2 + t}{4\nu}. \quad (9)$$

Performing the k_z -integration leads to:

$$F^{(b)} = \frac{i}{2\sqrt{2\pi}} \int \frac{d^2k_\perp}{(2\pi)^2} dz \Theta(-z) S_{df}^{jj'}(\mathbf{k}_\perp, z) e^{i\Delta_h z} \\ \times f^{\gamma^*p \rightarrow hp}\left(\frac{\mathbf{l}_\perp}{2} - \mathbf{k}_\perp\right) f^{hn \rightarrow Vn}\left(\frac{\mathbf{l}_\perp}{2} + \mathbf{k}_\perp\right) + (p \leftrightarrow n), \quad (10)$$

where the transition form factor in the mixed representation is defined via:

$$S_{df}^{jj'}(\mathbf{k}_\perp, k_z) = \frac{1}{\sqrt{2\pi}} \int dz S_{df}^{jj'}(\mathbf{k}_\perp, z) e^{-ik_z z}. \quad (11)$$

Adding explicitly the contribution where first the neutron and then the proton interacts gives:

$$F^{(b)} = \tilde{F}^{(b)} + \Delta F^{(b)}, \quad (12)$$

with:

$$\tilde{F}^{(b)} = \frac{i}{2} \int \frac{d^2k_\perp}{(2\pi)^2} S_{df}^{jj'}(\mathbf{k}_\perp, -\Delta_h) f^{\gamma^*p \rightarrow hp}\left(\frac{\mathbf{l}_\perp}{2} - \mathbf{k}_\perp\right) f^{hn \rightarrow Vn}\left(\frac{\mathbf{l}_\perp}{2} + \mathbf{k}_\perp\right), \quad (13)$$

$$\Delta F^{(b)} = \frac{i}{2\sqrt{2\pi}} \int \frac{d^2k_\perp}{(2\pi)^2} dz \Theta(z) \times \quad (14) \\ \left[S_{df}^{jj'}(-\mathbf{k}_\perp, z) e^{-i\Delta_h z} f^{\gamma^*n \rightarrow hn}\left(\frac{\mathbf{l}_\perp}{2} - \mathbf{k}_\perp\right) f^{hp \rightarrow Vp}\left(\frac{\mathbf{l}_\perp}{2} + \mathbf{k}_\perp\right) \right. \\ \left. - S_{df}^{jj'}(\mathbf{k}_\perp, z) e^{i\Delta_h z} f^{\gamma^*p \rightarrow hp}\left(\frac{\mathbf{l}_\perp}{2} - \mathbf{k}_\perp\right) f^{hn \rightarrow Vn}\left(\frac{\mathbf{l}_\perp}{2} + \mathbf{k}_\perp\right) \right].$$

Since $\Delta F^{(b)}$ is only a small correction to $\tilde{F}^{(b)}$ we neglect in the former the difference between the proton and neutron amplitudes. For specific target polarizations the form factor $S_{df}^{jj'}$ is invariant under rotations in the transverse plane, i.e. $S_{df}^{jj'}(-\mathbf{k}_\perp, z) = S_{df}^{jj'}(\mathbf{k}_\perp, z)$. Then one obtains:

$$\Delta F^{(b)} = -\frac{1}{\sqrt{2\pi}} \int \frac{d^2k_\perp}{(2\pi)^2} \Delta S_{df}^{jj'}(\mathbf{k}_\perp, -\Delta_h) f^{\gamma^*N \rightarrow hN}\left(\frac{\mathbf{l}_\perp}{2} - \mathbf{k}_\perp\right) f^{hN \rightarrow VN}\left(\frac{\mathbf{l}_\perp}{2} + \mathbf{k}_\perp\right), \quad (15)$$

with

$$\Delta S_{df}^{jj'}(\mathbf{k}_\perp, -\Delta_h) = \int dz \Theta(z) S_{df}^{jj'}(\mathbf{k}_\perp, z) \sin(-\Delta_h z). \quad (16)$$

It is important to note that the double scattering amplitude in Eq.(12) explicitly includes the energy and momentum dependence of the longitudinal photon interaction length. It

therefore differs from the corresponding amplitude derived for hadron-deuteron scattering processes [18]. In addition, the derived single (2) and double scattering amplitude (12) account for the recoil of the final pn system which is not included in the conventional approach of Ref. [18]. The results of the latter can be obtained from Eqs.(2) and (12) after neglecting recoil effects by taking the limit $\Delta_h \rightarrow 0$ and replacing $\gamma^* \rightarrow h = V$.

Collecting the results for single (2) and double scattering (12) and summing over all possible intermediate hadronic states h gives for the vector meson production amplitude:

$$\begin{aligned}
F_{df}^{jj'} &= F^{(a)} + F^{(b)} = f^{\gamma^*N \rightarrow VN}(\mathbf{l}) \left[S_{df}^{jj'} \left(-\frac{\mathbf{l}_\perp}{2}, \frac{l_-}{2} \right) + S_{df}^{jj'} \left(\frac{\mathbf{l}_\perp}{2}, -\frac{l_-}{2} \right) \right] \\
&+ \frac{i}{2} \sum_h \int \frac{d^2k_\perp}{(2\pi)^2} f^{\gamma^*N \rightarrow hN} \left(\frac{\mathbf{l}_\perp}{2} - \mathbf{k}_\perp \right) f^{hN \rightarrow VN} \left(\frac{\mathbf{l}_\perp}{2} + \mathbf{k}_\perp \right) \\
&\quad \times \left[S_{df}^{jj'}(\mathbf{k}_\perp, -\Delta_h) + \frac{2i}{\sqrt{2\pi}} \Delta S_{df}^{jj'}(\mathbf{k}_\perp, -\Delta_h) \right]. \tag{17}
\end{aligned}$$

To investigate the production process in different kinematic domains it is useful to express the transition amplitude $f^{\gamma^*N \rightarrow hN}$ in a hadronic basis for the incoming virtual photon (see e.g. [8,12]):

$$f^{\gamma^*N \rightarrow hN} = \sum_{h'} \frac{\langle 0 | \epsilon_{\gamma^*} \cdot J^{em} | h' \rangle d\tau_{h'}}{E_{h'} - \nu} f^{h'N \rightarrow hN}, \tag{18}$$

where ϵ_{γ^*} is the polarization vector of the virtual photon and J^{em} is the electromagnetic current. $E_{h'}$ denotes the energy of the intermediate hadronic state h' and $d\tau_{h'}$ stands for the corresponding phase-space factor. The hadronic representation in (18) is based on the existence of a spectral representation for the electromagnetic scattering operator [19]. Inserting Eq.(18) into the amplitude (17) leads to:

$$\begin{aligned}
F_{df}^{jj'} &= \sum_{h'} \frac{\langle 0 | \epsilon_{\gamma^*} \cdot J^{em} | h' \rangle d\tau_{h'}}{E_{h'} - \nu} f^{h'N \rightarrow VN}(\mathbf{l}) \left[S_{df}^{jj'} \left(-\frac{\mathbf{l}_\perp}{2}, \frac{l_-}{2} \right) + S_{df}^{jj'} \left(\frac{\mathbf{l}_\perp}{2}, -\frac{l_-}{2} \right) \right] \\
&+ \frac{i}{2} \sum_{h',h} \int \frac{d^2k_\perp}{(2\pi)^2} \frac{\langle 0 | \epsilon_{\gamma^*} \cdot J^{em} | h' \rangle d\tau_{h'}}{E_{h'} - \nu} f^{h'N \rightarrow hN} \left(\frac{\mathbf{l}_\perp}{2} - \mathbf{k}_\perp \right) f^{hN \rightarrow VN} \left(\frac{\mathbf{l}_\perp}{2} + \mathbf{k}_\perp \right) \\
&\quad \times \left[S_{df}^{jj'}(\mathbf{k}_\perp, -\Delta_h) + \frac{2i}{\sqrt{2\pi}} \Delta S_{df}^{jj'}(\mathbf{k}_\perp, -\Delta_h) \right]. \tag{19}
\end{aligned}$$

Although the amplitude in Eq.(19) cannot be calculated explicitly in a model independent way, it reveals three different energy domains of the production process.

The first region corresponds to intermediate photon energies and low momentum transfers $Q^2 \lesssim 1 \text{ GeV}^2$. Here contributions to the scattering amplitude (19) from intermediate states h' with large invariant masses $m_{h'}'$ are suppressed by large energy denominators:

$$E_{h'} - \nu \approx \frac{m_{h'}'^2 + Q^2}{2\nu}. \tag{20}$$

The possible restriction to small mass intermediate states leads to the vector meson dominance (VMD) model (for a review see e.g. Ref. [2]).

At high energies but fixed Q^2 contributions from intermediate hadronic states with large masses ($m_{h'}^2 \gg Q^2$) are important. They are usually described through the triple reggeon formalism [20].

The third kinematic domain corresponds to large momentum transfers, $Q^2 \gg 1 \text{ GeV}^2$, and small values of $x \ll 1/4MR_A$, where R_A is the radius of the target nucleus. Here it is legitimate to use closure over intermediate hadronic states h and h' and substitute in (19) the sums over hadronic states by a quark-gluon wave packet which can be calculated within perturbative QCD. For example in the case of longitudinally polarized photons at large Q^2 short distance dominance leads to the interaction of a color-dipole, quark-antiquark pair with small transfer size [3,6,21,22].

We want to investigate the Q^2 -dependence of the re-scattering amplitude in the kinematic domain $0 < Q^2 < 10 \text{ GeV}^2$ and moderate photon energies, such that closure over intermediate hadronic states as discussed above is not applicable. To account for effects which result from the kinematic dependence of the effective longitudinal interaction length we perform a baseline calculation within the framework of vector meson dominance. We then consider processes which are sensitive to re-scattering, but to a good approximation independent from the initial production process. Thus we obtain signatures for color coherence and avoid uncertainties which result from modeling the transition amplitudes for intermediate hadronic states.

III. COHERENT VECTOR MESON PRODUCTION

In the remainder of the paper we focus on the coherent production of vector mesons, i.e. the deuteron target stays intact. Note that our results can be easily generalized to vector meson production with deuteron break-up, as well as to exclusive pion production processes, like $\gamma^* + d \rightarrow \pi^- + pp$, where color coherence effects can also be explored [23].

Before we discuss specific reactions suited to investigate re-scattering processes, we remind on basic features of the leptoproduction cross section and vector meson dominance.

A. Differential cross section and vector meson dominance

The coherent vector meson production amplitude in (virtual) photon-deuteron interactions can be obtained from Eqs.(17) and (19) if one requires the final pn state to be a deuteron ($f = d$). If the polarization of the vector meson is not observed the leptoproduction cross section reads:

$$\frac{d\sigma_{ld \rightarrow lVd}^{s,mm'}}{dQ^2 d\nu dt d\phi} = \frac{\Gamma_V}{32\pi^2} L^{\mu\nu} \left(F_\mu^\rho F_{\nu\rho}^\dagger \right)^{s,mm'}. \quad (21)$$

Here we have specified the spin quantum numbers which were labeled in the previous section by j and j' . The index s specifies the deuteron spin quantization axis and $m, m' = 0, \pm 1$ are the corresponding spin projections of the target before and after the scattering, respectively. The four-momenta of the incoming and scattered lepton are $k_e^\mu = (E_e, \mathbf{k}_e)$ and $k_e^{\mu'} = (E_e', \mathbf{k}_e')$. $L^{\mu\nu} = \frac{1}{2} \text{Tr}(\hat{k}_e' \gamma^\mu \hat{k}_e \gamma^\nu)$ stands for the leptonic tensor with $\hat{k} = k_\mu \gamma^\mu$, neglecting terms proportional to the lepton mass.

Furthermore, ϕ denotes the angle between the lepton scattering plane defined by the momenta \mathbf{k}_e and \mathbf{k}'_e , and the vector meson production plane determined by the photon and vector meson momenta \mathbf{q} and \mathbf{k}_V . Finally, Γ_V is related to the flux of the virtual photon:

$$\Gamma_V = \frac{\alpha_{em}}{2\pi} \frac{K}{Q^2} \frac{1}{E_e^2} \frac{1}{1-\epsilon}, \quad (22)$$

where $\alpha_{em} = 1/137$ is the electromagnetic coupling constant, $K = \nu(1-x)$, and $\epsilon = (4E_e E'_e - Q^2)/(2(E_e^2 + E_e'^2) + Q^2)$ specifies the photon polarization. Multiplying the tensor $F_{\mu\rho}$ in (21) with the polarization vectors of the incident photon and the produced vector meson yields the photoproduction amplitude $F_d = \epsilon_{\gamma^*}^\mu F_{\mu\nu} \epsilon_V^\nu$ from Eqs.(17) and (19).

The differential cross section (21) is often written in terms of structure functions with definite helicity [24]. For this purpose the following photon polarization vectors are introduced:

$$\epsilon_{\pm}^\mu = \mp \frac{1}{\sqrt{2}} (0, 1, \pm i, 0), \quad (23)$$

$$\epsilon_0^\mu = \frac{1}{\sqrt{Q^2}} \left(\sqrt{\nu^2 + Q^2}, \mathbf{0}_\perp, \nu \right). \quad (24)$$

Note that in the above definitions the z -axis has been chosen parallel to the photon momentum. The differential cross section can then be written as:

$$\frac{d\sigma_{ld \rightarrow lVd}^{s,mm'}}{dQ^2 d\nu dt d\phi} = \frac{\Gamma_V}{32\pi^2} \left(\sigma_T^{s,mm'} + \epsilon \sigma_L^{s,mm'} - \epsilon \cos(2\phi) \sigma_{TT}^{s,mm'} + \sqrt{\epsilon(1+\epsilon)} \cos(\phi) \sigma_{TL}^{s,mm'} \right). \quad (25)$$

Here the different structure functions are defined as:

$$\begin{aligned} \sigma_T^{s,mm'} &= \frac{1}{2} \left(F_+^\rho F_{+\rho}^\dagger + F_-^\rho F_{-\rho}^\dagger \right)^{s,mm'}, \\ \sigma_L^{s,mm'} &= \left(F_0^\rho F_{0\rho}^\dagger \right)^{s,mm'}, \\ \sigma_{TT}^{s,mm'} &= \left(\text{Re} F_+^\rho F_{-\rho}^\dagger \right)^{s,mm'}, \\ \sigma_{TL}^{s,mm'} &= \left(\text{Re} F_0^\rho (F_{+\rho} - F_{-\rho})^\dagger \right)^{s,mm'}, \end{aligned} \quad (26)$$

where $F_{\lambda\rho}^{s,mm'} = \epsilon_\lambda^\mu F_{\mu\rho}^{s,mm'}$, with the helicity $\lambda = 0, +, -$.

The leptoproduction cross section (25) is connected to the virtual photoproduction cross section via:

$$\frac{d\sigma_{\gamma^* d \rightarrow Vd}^{s,mm'}}{dt d\phi} = \frac{1}{\Gamma_V} \frac{d\sigma_{ld \rightarrow lVd}^{s,mm'}}{dQ^2 d\nu dt d\phi}. \quad (27)$$

If the cross section is integrated over the azimuthal angle ϕ the helicity flip structures σ_{TT} and σ_{TL} drop out and we end up with:

$$\frac{d\sigma_{\gamma^* d \rightarrow Vd}^{s,mm'}}{dt} = \frac{1}{16\pi} \left(\sigma_T^{s,mm'} + \epsilon \sigma_L^{s,mm'} \right). \quad (28)$$

It is an experimental fact that in vector meson production from free nucleons at small $|t|$ the helicity of the vector meson is, to a good approximation, equal to the helicity of the incoming photon [25]. Assuming this so-called s -channel helicity conservation for both amplitudes $f^{\gamma^*N \rightarrow hN}$ and $f^{hN \rightarrow VN}$ in (17) yields³ $\sigma_{TT} = \sigma_{TL} = 0$. The helicity conserving structures σ_T and σ_L in (26) can be calculated from the photon-deuteron amplitude in Eq.(17) if the nucleon amplitudes $f^{\gamma^*N \rightarrow hN}$ and $f^{hN \rightarrow VN}$ are specified. Here this is done within the framework of the vector meson dominance model, where the electromagnetic current which enters in (19) is represented by vector meson fields (see e.g. [2] and references therein):

$$J_\mu^{em} = \sum_V \frac{\sqrt{\pi\alpha_{em}m_V^2}}{g_V} \delta(m_{h'}^2 - m_V^2) V_\mu, \quad (29)$$

where V_μ ($V = \rho, \omega, \phi$) stands for the vector meson field with invariant mass m_V and coupling constant g_V . Combining Eqs.(18),(20) and (29) yields the vector meson production amplitude for transversely polarized photons:

$$f^{\gamma_T^*N \rightarrow VN} = \sum_{V'} \frac{\sqrt{\alpha_{em}\pi}}{g_{V'}} \frac{m_{V'}^2}{m_{V'}^2 + Q^2} f^{V'_T N \rightarrow VN} \approx \frac{\sqrt{\alpha_{em}\pi}}{g_V} \frac{m_V^2}{m_V^2 + Q^2} f^{V_T N \rightarrow VN}. \quad (30)$$

In the following we neglect off-diagonal transitions $V'N \rightarrow VN$. In analogy with the suppression of inelastic diffraction to π' states in diffractive pion-nucleon scattering, $\pi N \rightarrow XN$, they are expected to be small. Furthermore, since the deuteron is an isosinglet the diagonal approximation is justified in the kinematic region where vector meson dominance is applicable at least for coherent ρ -production due to the different isospin of the ρ - compared to the ω - and ϕ -meson. Consequently, the diagonal approximation is exact for single scattering contributions while off-diagonal contributions are expected to be small for double scattering.⁴

In vector meson dominance the production amplitude for longitudinally polarized virtual photons is related to the corresponding amplitude for transverse photons by (see e.g. [24]):

$$f^{\gamma_L^*N \rightarrow VN} = \xi \frac{\sqrt{Q^2}}{m_V} f^{\gamma_T^*N \rightarrow VN}, \quad (31)$$

where the ratio of the longitudinal to transverse vector meson-nucleon amplitude is denoted by $\xi = f^{V_L N \rightarrow VN} / f^{V_T N \rightarrow VN}$.

It remains to fix the amplitude $f^{\gamma_T^*N \rightarrow VN}$. We concentrate on diffractive ρ -production and use for explicit calculations the parameterization:

$$f^{\gamma_T^*N \rightarrow VN} = \sigma_{\gamma^*\rho}(i + \alpha) e^{\frac{B(Q^2)}{2}t}, \quad (32)$$

³The quality of s -channel helicity conservation can be investigated according to (25) by out-of-plane measurements.

⁴ Note that at large Q^2 non-diagonal transitions to states with invariant masses $m_h^2 \lesssim Q^2$ are important and are supposed to lead to color transparency.

where $t \approx -\mathbf{k}_t^2$. In real photoproduction at $\nu = 17 \text{ GeV}$ one finds typically $\sigma_{\gamma\rho} \approx 68 \mu\text{b}$ [2]. For the slope $B(Q^2)$ we use the empirical values [2,17]: $B(Q^2 < 1 \text{ GeV}^2) = 7 \text{ GeV}^{-2}$, $B(1 \text{ GeV}^2 < Q^2 < 2 \text{ GeV}^2) = 6 \text{ GeV}^{-2}$ and $B(2 \text{ GeV}^2 < Q^2 < 10 \text{ GeV}^2) = 5 \text{ GeV}^{-2}$. The ratio of real to imaginary part of the production amplitude in (32) is fixed at $\alpha \approx -0.2$, and we use $\xi^2 = 0.5$ [2]. The ρN -amplitude is then obtained from Eq.(30) using the slope $B \approx 8 \text{ GeV}^{-2}$. Note that at intermediate energies the real part of the scattering amplitudes for proton and neutron targets are not exactly the same. We omit this difference since coherent vector meson production from deuterium is dominated by isospin averaged amplitudes.

In the following we consider the photoproduction cross section (28). It is determined by the square of the production amplitude Eq.(17). In the framework of vector meson dominance the latter is given explicitly in Appendix B.

B. Evidence for double scattering

Our main goal is to find kinematic domains where the vector meson production cross section is sensitive to the re-scattering amplitude (Fig.1b). First however let us recall that there is experimental evidence for double scattering which is theoretically well understood. In Fig.2 we show data on coherent photoproduction of ρ -mesons from unpolarized deuterium measured at SLAC [26,27] for a photon energy $\nu = 12 \text{ GeV}$. We compare the experimental data with results obtained from Eqs.(28) and (30).

It is evident that vector meson dominance successfully describes the measured data. Furthermore, one observes for $-t \gtrsim 0.4 \text{ GeV}^2$ significant contributions from double scattering. Here the single scattering (Born) contribution as well as the contribution from the interference of single and double scattering become less important. At $-t > 0.6 \text{ GeV}^2$ the differential cross section is entirely controlled by double scattering.

The importance of double scattering at large transferred momenta can easily be understood investigating the corresponding amplitudes in (2) and (12). At large $|t|$ single scattering is suppressed through the large momentum transfer which enters in the deuteron form factor. In double scattering, however, the transferred momentum is shared between both interacting nucleons. Therefore re-scattering probes the deuteron form factor at moderate momenta even at large $|t|$. In the present analysis we restrict ourselves to $|t| < M_d^2$ where corrections due to relativistic components in the deuteron wave function are expected to be small.

In the following we discuss further options to probe double scattering contributions. Especially polarized deuterium targets provide various possibilities for their investigation as we will demonstrate. Before focusing on signatures for color coherence we investigate effects sensitive to the characteristic longitudinal interaction length of the production process.

C. Finite longitudinal interaction length

As already mentioned in the introduction high-energy (virtual) photon-induced processes are dominated by contributions from large longitudinal space-time intervals which increase with the energy of the incident photon. For coherent vector meson production the characteristic distances can be extracted from the production amplitude in Eq.(17) after a Fourier

transformation into coordinate space. The obtained length scales are to a good approximation inversely proportional to the longitudinal momentum transfers which enter in the form factors in Eq.(17). For single scattering one finds:

$$\delta_z^{(a)} \sim \left| \frac{1}{l_-} \right| = \frac{2\nu}{Q^2 + m_V^2 - t}, \quad (33)$$

while for double scattering one gets:

$$\delta_z^{(b)} \sim \left| \frac{1}{-2\Delta_V} \right| = \left| \frac{2\nu}{Q^2 + m_V^2 + t} \right|. \quad (34)$$

Note that if the deuteron recoil is neglected the longitudinal interaction length for single scattering reads:

$$\delta_z^{(a)} \sim \left| \frac{1}{l_z} \right| = \frac{2\nu}{Q^2 + m_V^2 - t - \nu t/M_d} \xrightarrow{\nu \rightarrow \infty} 2M_d/|t|, \quad (35)$$

which for $t \neq 0$ becomes a constant at high energies. This contradicts our basic understanding of high-energy photon-induced processes being controlled by longitudinal distances which increase with the photon energy ν [7–10].

At intermediate energies where characteristic longitudinal interaction distances are of the order of the target size, $\delta_z^{(a)}, \delta_z^{(b)} \sim \langle r^2 \rangle_d^{1/2}$, a strong energy dependence of the cross section is expected. In momentum space this can be traced back to the sensitive momentum dependence of the deuteron form factor which enters the production amplitude (17).

For a quantitative investigation we consider the ρ -meson photoproduction cross section (28) for an unpolarized deuterium target using proper longitudinal interaction distances (33, 34) as they appear in the scattering amplitude (17), normalized by the cross section calculated in the limit $\delta_z^{(a)}, \delta_z^{(b)} \rightarrow \infty$:

$$R_{\delta_z} = \frac{d\sigma_{\gamma^* d \rightarrow \rho d}}{dt} \bigg/ \frac{d\sigma_{\gamma^* d \rightarrow \rho d}}{dt} (l_- = \Delta_\rho = 0). \quad (36)$$

In Fig.3 we show R_{δ_z} for photo- and leptoproduction in the kinematic domain of TJNAF [28]. Here the characteristic longitudinal interaction distance for single scattering is typically of the order of the deuteron size. For example at $\nu = 4 \text{ GeV}$ and $t = -0.2 \text{ GeV}^2$, one finds $\delta_z^{(a)} \approx 2 \text{ fm}$. Consequently we observe at small $-t \lesssim 0.4 \text{ GeV}^2$, where the Born term dominates, a strong dependence of the production cross section on ν and Q^2 . Indeed at $t \sim -0.1 \text{ GeV}^2$ an increase in the photon energy⁵ from 3 GeV to 6 GeV leads to a 15% rise of R_{δ_z} . In leptoproduction at $t \sim -0.1 \text{ GeV}^2$ and $\nu = 6 \text{ GeV}$ an increase of Q^2 from 0.5 GeV^2 to 2 GeV^2 yields a decrease of R_{δ_z} by approximately 50%. At large $-t > 0.7 \text{ GeV}^2$, where double scattering dominates, only minor variations of the production cross section occur since here smaller proton-neutron distances are probed.

If vector meson production is considered at higher photon energies effects from finite longitudinal interaction distances occur too, however at larger values of Q^2 . As an example

⁵Note that the validity of vector meson dominance [2] demands a minimal photon energy $\nu \gtrsim 3 \text{ GeV}$.

we present in Fig.4 the cross section ratio R_{δ_z} for $\nu = 30 \text{ GeV}$ and $Q^2 = (2 - 10) \text{ GeV}^2$. This kinematic region is accessible at HERMES [29]. Although at $Q^2 > 2 \text{ GeV}^2$ vector meson dominance does not describe the Q^2 -dependence of the nucleon production amplitude $f_{\gamma^* N \rightarrow VN}$ properly, in the ratio R_{δ_z} to a good approximation any Q^2 -dependence of the single scattering amplitude drops out. Therefore in the domain where the Born contribution dominates, i.e. at $-t \lesssim 0.4 \text{ GeV}^2$, the presented results should be reasonable. As before we observe at $t \sim -0.1 \text{ GeV}^2$ a strong rise of the production cross section for decreasing values of Q^2 . Double scattering, which dominates the cross section at large $|t|$, will depend sensitively on Q^2 due to color coherence effects. Therefore at large $Q^2 > 2 \text{ GeV}^2$ and $-t > 0.4 \text{ GeV}^2$ the cross section ratio R_{δ_z} calculated within vector meson dominance should be considered as a baseline estimate assuming color coherence effects to be absent.

Coherent vector meson production from polarized deuterons provides further possibilities to investigate effects due to a change of the characteristic longitudinal interaction length. If the polarization of the scattered deuteron is not observed the Born cross section is proportional to the deuteron density matrix (see Appendix B and C):

$$\rho^{s,m} \left(\frac{\mathbf{l}_\perp}{2}, -\frac{l_-}{2} \right) = \sum_{m'} S_d^{s,mm'} \left(\frac{\mathbf{l}_\perp}{2}, -\frac{l_-}{2} \right) S_d^{s,mm'} \left(\frac{\mathbf{l}_\perp}{2}, -\frac{l_-}{2} \right)^\dagger. \quad (37)$$

Note that l_- enters on the left- and right-hand side of Eq.(37) as a consequence of the recoil of the final state (Appendix A). Choosing the spin quantization axis parallel to the photon momentum \mathbf{q} , which we denote by $s = 1$, one finds for $m = 0$ (C3):

$$\rho^{1,0} \left(\frac{\mathbf{l}_\perp}{2}, -\frac{l_-}{2} \right) = F_C^2(\tilde{l}/2) + \left[\frac{3l_-^2}{\tilde{l}^2} - 1 \right] \sqrt{2} F_C(\tilde{l}/2) F_Q(\tilde{l}/2) + \left[\frac{3l_-^2}{\tilde{l}^2} + 1 \right] \frac{F_Q^2(\tilde{l}/2)}{2}, \quad (38)$$

where $\tilde{l}^2 = \mathbf{l}_\perp^2 + l_-^2$. F_C and F_Q are the deuteron monopole and quadrupole form factors as defined in the appendix (C2). For the Paris potential [30] they are shown in Fig.5. In the limit $l_- = 0$ the density matrix reduces to:

$$\rho^{1,0} \left(\frac{\mathbf{l}_\perp}{2}, 0 \right) = \left(F_C(l_\perp/2) - \frac{1}{\sqrt{2}} F_Q(l_\perp/2) \right)^2. \quad (39)$$

with $l_\perp = |\mathbf{l}_\perp|$. From Fig.6 we observe that $\rho^{1,0}(l_\perp/2, 0) = 0$ for $l_\perp \approx 0.7 \text{ GeV}$, leading to the disappearance of the single scattering contribution. Consequently for $l_- \ll \sqrt{-t}/3$ the production cross section is dominated by double scattering contributions at $t \approx -l_\perp^2 \approx -0.5 \text{ GeV}^2$. We therefore expect in this region of t a strong energy dependence of the Born contribution since $l_- \sim 1/\delta_z^{(a)} \sim 1/\nu$.

In Fig.7 we show the ρ -meson photoproduction cross section (28)

$$\frac{d\sigma_{\gamma^* d \rightarrow \rho d}^{1,0}}{dt} = \sum_{m'} \frac{d\sigma_{\gamma^* d \rightarrow \rho d}^{1,0m'}}{dt}. \quad (40)$$

for different photon energies. We indeed observe a significant energy dependence of the Born contribution at $t \approx -0.5 \text{ GeV}^2$. Combined with double scattering it leads to a decrease of the production cross section at $t \approx -0.35 \text{ GeV}^2$ of more than two orders of magnitude if the photon energy rises from $\nu = 3 \text{ GeV}$ to 10 GeV .

D. Color coherence effects at large $|t|$

In Sec.III B we have demonstrated that within the framework of vector meson dominance double scattering dominates the coherent production cross section at $-t > 0.6 \text{ GeV}^2$. However, as outlined in the introduction, at large $Q^2 \gg 1 \text{ GeV}^2$ the hadronic state which is formed in the interaction of the virtual photon with a nucleon is in general not a vector meson as in vector meson dominance, but a quark-gluon wave packet with a characteristic transverse size $b_{ej} \sim 1/Q$. If the energy of this ejectile is large enough, such that its formation time $\tau_f \approx 2\nu/\delta m_V^2$ exceeds the target size, it will be the ejectile which re-scatters from the second nucleon. One therefore expects double scattering to vanish at $Q^2 \gg 1 \text{ GeV}^2$ and $\nu > \langle r^2 \rangle_d^{1/2} \delta m_V^2 / 2 \approx 10 \text{ GeV}$. This color coherence or color transparency effect can be investigated through the Q^2 -dependence of the vector meson production cross section in kinematic regions where it is most sensitive to re-scattering. However, for this purpose it is mandatory to account for eventual modifications due to a change of the characteristic longitudinal interaction lengths $\delta_z^{(a)}$ and $\delta_z^{(b)}$ from Eqs.(33,34). Or, even better, the kinematics should be chosen such that these length scales stay constant.

In Fig.8 we present a baseline calculation for coherent ρ -production from unpolarized deuterons within vector meson dominance. For different values of Q^2 the corresponding photon energies ν are chosen such that $x = 0.1$. At large values of ν we then have $\delta_z^{(a)} \approx \delta_z^{(b)} \approx 1/Mx \approx 2 \text{ fm}$. We normalize the production cross section by the cross section taken at $t = t_{min}$ and show the ratio:

$$R = \frac{d\sigma_{\gamma^* d \rightarrow \rho d}}{dt} \bigg/ \frac{d\sigma_{\gamma^* d \rightarrow \rho d}}{dt}(t = t_{min}). \quad (41)$$

Note that in R any Q^2 - and ν -dependence of the initial photoproduction process cancels. In addition we show in Fig.8 the corresponding cross section ratio R_{Born} which accounts for single scattering only. We observe that at large $-t \gtrsim (0.8 - 1) \text{ GeV}^2$ the full production cross section is approximately a factor 2.5–5 larger than the Born contribution. This difference is the maximal effect which can be caused by color coherence: at small $Q^2 < 1 \text{ GeV}^2$ vector meson dominance is applicable and the hadronic state which re-scatters can be represented by a soft vector mesons. Consequently the cross section ratio should be identical to R . However if, as a consequence of color coherence, double scattering is absent at large Q^2 and large ν , only single scattering contributes to the production cross section and yields the ratio R_{Born} .

The difference between the Born cross section and the full production cross section in absence of color coherence can be enhanced, if one considers the ratio of the cross sections at large and moderate $|t|$. In absence of color coherence vector meson production at large $|t|$ is dominated by double scattering and the overall cross section is larger than the Born contribution. However at moderate $t \sim -0.4 \text{ GeV}^2$ the interference of the double and single scattering amplitude is important and leads to an overall production cross section being smaller than the Born term. Taking the ratio of both gives an enhanced sensitivity to the double scattering contribution and thus to eventual color coherence effects. Furthermore in such a cross section ratio any Q^2 -dependence, apart from being caused by color coherence, cancels to a large extend. In Fig.9 we present the ratio of the ρ -meson production cross sections from unpolarized deuterons at $x = 0.1$ for $t = -0.4 \text{ GeV}^2$ and $t = -0.8 \text{ GeV}^2$. The

Born cross section and the full vector meson dominance calculation differ by a factor of 4, leaving reasonable room for an investigation of color coherence.

E. Color coherence at moderate $|t|$

At moderate values of $|t|$ vector meson production from unpolarized deuterons is largely dominated by the Born contribution. For polarized targets, however, even here kinematic windows exist where the Born contribution is small and the production cross section becomes sensitive to re-scattering.

We first consider a deuteron target with spin projection $m = 0$ along the photon momentum \mathbf{q} (labeled as previously by $s = 1$). For such a polarization we have found in Sec.III C a dip in the Born cross section at $t \approx -0.5 \text{ GeV}^2$. The latter, however, depends strongly on l_- or, equivalently, the longitudinal interaction length $\delta_z^{(a)}$. To suppress this dependence we consider the ratio:

$$R^{1,0} = \frac{d\sigma_{\gamma^*d \rightarrow \rho d}^{1,0}}{dt} \bigg/ \frac{d\sigma_{\gamma^*d \rightarrow \rho d}^{1,0}}{dt} (t = t_{min}), \quad (42)$$

for various Q^2 but at fixed values of x . In Fig.10 we compare $R^{1,0}$ with the corresponding cross section ratio $R_{Born}^{1,0}$ obtained from single scattering only. As expected, at small x the Born contribution develops a minimum at $t \approx -0.5 \text{ GeV}^2$. Here we find at $x = 0.05$ an order of magnitude difference between the Born and the full vector meson dominance cross section. At $x = 0.001$ the difference is even larger than two orders of magnitude. Therefore an investigation of the Q^2 -dependence of the cross section ratio $R^{1,0}$ in the region $t \approx -0.5 \text{ GeV}^2$ can serve as a tool to investigate double scattering contributions to vector meson production and thus color coherence.

An even more interesting choice for the target polarization is to take the spin projection $m = 0$ perpendicular to the vector meson production plane, i.e. parallel to $\boldsymbol{\kappa} = \mathbf{q} \times \mathbf{l}$, which we label as $s = 2$. The corresponding deuteron density matrix for the Born cross section reads (C3):

$$\rho^{2,0} \left(\frac{\mathbf{l}_\perp}{2}, -\frac{l_-}{2} \right) = \left(F_C^2(\tilde{l}/2) - \frac{1}{\sqrt{2}} F_Q(\tilde{l}/2) \right)^2, \quad (43)$$

irrespective of the magnitude of the longitudinal momentum transfer l_- . Consequently, for this target polarization a node in the Born contribution occurs for $\tilde{l} = 0.7 \text{ GeV}$, which again corresponds for the large energies considered approximately to $t \approx -0.5 \text{ GeV}^2$. In Fig.11 we show the t -dependence of the cross section ratio $R^{2,0}$ defined similar to Eq.(42). The observed node in the Born contribution leads to a perfect window for an investigation of double scattering.

Finally we consider the cross section for tensor polarization normalized by the unpolarized production cross section:

$$A_d = \frac{d\sigma^{2,1}/dt + d\sigma^{2,-1}/dt - 2d\sigma^{2,0}/dt}{d\sigma/dt}, \quad (44)$$

where the spin quantization axis is taken parallel to $\boldsymbol{\kappa}$. In comparison to the corresponding asymmetry for the Born contribution we find a significant sensitivity to double scattering at $-t > 0.6 \text{ GeV}^2$ as demonstrated in Fig.12.

IV. CONCLUSIONS

Coherent leptonproduction of vector mesons from deuterium provides unique possibilities to investigate the characteristic longitudinal interaction length in high-energy photon-induced processes, and to search for color coherence phenomena. We have presented a derivation of the corresponding amplitudes including the recoil of the scattered deuteron. The latter is neglected in common derivations based on the Glauber multiple scattering formalism, but turns out to be important in the case of non-forward production processes from light nuclei.

We have identified kinematic regions where vector meson production is influenced significantly by variations of the longitudinal interaction length of the photon which depends in a specific way on the photon energy and the momentum transfer. Several possibilities for an investigation of the latter in the kinematic domain of TJNAF and HERMES are outlined.

A further issue of this work was the identification of kinematic windows where the vector meson production cross section is most sensitive to re-scattering contributions. Here the propagation of small size quark-gluon configurations, which are initially produced in high-energy lepton-nucleon interactions at large Q^2 , can be studied. We found promising signatures for color coherence in the kinematic domain of HERMES. For unpolarized deuteron targets they involve large momentum transfers $-t \gtrsim 0.6 \text{ GeV}^2$, while for polarized targets re-scattering can be investigated already at moderate $-t \sim 0.5 \text{ GeV}^2$.

ACKNOWLEDGMENTS

This work was supported in part by the German-Israeli Foundation Grant GIF -I-299.095, by the U.S. Department of Energy under Contract No. DE-FG02-93ER40771, by the National Science Foundation under Grants Nos. PHY-9511923 and PHY-9258270, and by the BMBF. M. Sargsian thanks the Alexander von Humboldt Foundation for support.

APPENDIX A: NUCLEAR RECOIL

In collisions at finite momentum transfer, $t = l^2 \neq 0$, a proper consideration of the longitudinal interaction length (33) and (34) goes beyond the conventional Glauber multiple scattering formalism which neglects nuclear recoil, i.e. the energy difference of the nucleus before and after the interaction (see e.g. [31]). As a consequence of the nuclear recoil the arguments of the scattered two-nucleon wave function in the amplitudes (2) and (4) depend on $l_- = l_0 - l_z$ instead of l_z as in the conventional Glauber approximation.

To clarify this issue recall that high-energy processes develop near the light-cone $|z - t| \approx 0$. Therefore they are naturally described in a light-cone description where the “-” and the transverse momentum components are conserved. As a result the deuteron wave function depends on the light-cone fraction of the deuteron momentum carried by the interacting nucleon, $\alpha = \frac{p_{d-} - p_{s-}}{p_{d-}}$, and on $\mathbf{p}_{s\perp}$, where p_d and $p_s^\mu = (p_{s0}, \mathbf{p}_{s\perp}, p_{sz})$ are the four-momenta of the deuteron and the spectator nucleon, respectively (Fig.1).

We consider the scattering process in a frame where the deuteron target is at rest. In addition we take the momentum of the virtual photon along the z -axis. The invariant mass of the initial two-nucleon system is:

$$M_i^2 = \frac{M^2 + \mathbf{p}_{s\perp}^2}{\alpha(1 - \alpha)}, \quad (\text{A1})$$

where M denotes the nucleon mass. For the single scattering process the mass of the two-nucleon system after the collision is:

$$M_f^2 = \frac{M^2 + \mathbf{p}_{s\perp}^2}{1 - \alpha_f} + \frac{M^2 + (\mathbf{l}_\perp - \mathbf{p}_{s\perp})^2}{\alpha_f} - \mathbf{l}_\perp^2 = \frac{M^2 + (\alpha_f \mathbf{l}_\perp - \mathbf{p}_{s\perp})^2}{\alpha_f(1 - \alpha_f)}. \quad (\text{A2})$$

where the final state, two-nucleon system is characterized by the variables:

$$\alpha_f = 1 - \frac{p_{s-}}{p_{d-} + l_-}, \quad \text{and} \quad \mathbf{p}_{f\perp} = \alpha_f \mathbf{l}_\perp - \mathbf{p}_{s\perp}. \quad (\text{A3})$$

On the other hand in the center of mass the invariant mass of the two-nucleon system before and after the interaction depends on the nucleon three-momentum only: $M_i^2 \approx 4(M^2 + \mathbf{p}_s^2)$ and $M_f^2 \approx 4(m^2 + \mathbf{p}_f^2)$. One then obtains in the non-relativistic limit:

$$\alpha = \frac{1}{2} \left(1 + \frac{p_{sz}}{M} \right), \quad \alpha_f = \frac{1}{2} \left(1 - \frac{p_{fz}}{M} \right), \quad \text{and} \quad p_{fz} = -p_{sz} - \frac{l_-}{2}. \quad (\text{A4})$$

Consequently the wave function of the target deuteron depends on p_{sz} and $\mathbf{p}_{s\perp}$, while in the wave function of the final two-nucleon system $p_{fz} = -p_{sz} - l_-/2$ and $\mathbf{p}_{f\perp} = -\mathbf{p}_{s\perp} + \frac{1}{2}(1 - \frac{p_{fz}}{M})\mathbf{l}_\perp \approx -\mathbf{p}_{s\perp} + \mathbf{l}_\perp/2$ enters. Note that $l_0 = \sqrt{M_f^2 + \mathbf{l}^2} - M_i$ corresponds to the recoil energy of the target.

Similar considerations can be repeated for the re-scattering process shown in Fig.1b. Here the light-cone momentum fraction of the nucleon in the intermediate state (after interacting with the photon) is:

$$\alpha_f = \frac{p_{d-} - p_{s-} + l_- - k_-}{p_{d-} + l_-} = \frac{p_{d-} - p_{s-} + l_- - k_-}{p_{d-}} \frac{p_{d-}}{p_{d-} + l_-}. \quad (\text{A5})$$

where $k^\mu = (k_0, \mathbf{k}) = p_s'^\mu - p_s^\mu$. In the non-relativistic limit one obtains:

$$\alpha_f \approx \frac{1}{2} \left(1 - \frac{p_{fz}}{M} \right) = \frac{1}{2} \left(1 + \frac{p_{sz}}{M} + \frac{l_-}{2M} - \frac{k_-}{M} \right). \quad (\text{A6})$$

We then get:

$$p_{fz} = -\frac{l_-}{2} + k_- - p_{sz}, \quad (\text{A7})$$

which corresponds to the longitudinal momentum component which enters the wave function in the double scattering amplitude in Eq.(4).

Note that in a light-cone approach which is necessary for a proper treatment of the production process at large momentum transfers $-t \geq (1-2) \text{ GeV}^2$ one needs to introduce relativistic deuteron wave functions. The corresponding light-cone transition form factor [32] naturally accounts for the recoil of the final nuclear system:

$$S(\mathbf{k}_\perp, l_-) = \int \frac{d\alpha}{\alpha(1-\alpha)} d^2k_\perp \psi_d(\alpha, \mathbf{p}_\perp) \psi_d(\alpha', \mathbf{p}_\perp - \mathbf{k}_\perp(1-\alpha')), \quad (\text{A8})$$

where $\alpha' = (\alpha + l_-/M)/(1 + \frac{l_-}{2M})$.

APPENDIX B: PHOTOPRODUCTION AMPLITUDES

Within the framework of vector meson dominance one obtains for the squared vector meson production amplitude for a deuterium target from Eqs.(2) and (12):

$$\begin{aligned} |F_d^{jj'}|^2 = |F_d^{sm,m'}|^2 = & F^{(a)} F^{(a)\dagger} + 2\text{Re} \left(F^{(a)} \tilde{F}^{(b)\dagger} \right) + \tilde{F}^{(b)} \tilde{F}^{(b)\dagger} + \\ & 2\text{Re} \left(F^{(a)} \Delta F^{(b)\dagger} \right) + 2\text{Re} \left(\tilde{F}^{(b)} \Delta F^{(b)\dagger} \right) + \Delta F^{(b)} \Delta F^{(b)\dagger}. \end{aligned} \quad (\text{B1})$$

The different terms are:

$$F^{(a)} F^{(a)\dagger} = 4 \left| f^{\gamma^* N \rightarrow VN}(\mathbf{l}) \right|^2 S_d^{s,mm'}(\mathbf{l}_\perp/2, -l_-/2)^2, \quad (\text{B2a})$$

$$\begin{aligned} 2\text{Re}(F^{(a)} \tilde{F}^{(b)\dagger}) = & -2\text{Im} \left\{ f^{\gamma^* N \rightarrow VN}(\mathbf{l}) S_d^{s,mm'}(\mathbf{l}_\perp/2, -l_-/2) \right. \\ & \times \left. \int \frac{d^2k_\perp}{(2\pi)^2} f^{\gamma^* N \rightarrow VN}(\mathbf{l}_\perp/2 - \mathbf{k}_\perp)^\dagger f^{VN \rightarrow VN}(\mathbf{l}_\perp/2 + \mathbf{k}_\perp)^\dagger S_d^{s,mm'}(\mathbf{k}_\perp, -\Delta_V) \right\}, \end{aligned} \quad (\text{B2b})$$

$$\begin{aligned} \tilde{F}^{(b)} \tilde{F}^{(b)\dagger} = & \frac{1}{4} \int \frac{d^2k_\perp}{(2\pi)^2} \frac{d^2k'_\perp}{(2\pi)^2} f^{\gamma^* N \rightarrow VN}(\mathbf{l}_\perp/2 - \mathbf{k}_\perp) f^{VN \rightarrow VN}(\mathbf{l}_\perp/2 + \mathbf{k}_\perp) \\ & \times f^{\gamma^* N \rightarrow VN}(\mathbf{l}_\perp/2 - \mathbf{k}'_\perp)^\dagger f^{VN \rightarrow VN}(\mathbf{l}_\perp/2 + \mathbf{k}'_\perp)^\dagger S_d^{s,mm'}(\mathbf{k}_\perp, -\Delta_V) S_d^{s,mm'}(\mathbf{k}'_\perp, -\Delta_V), \end{aligned} \quad (\text{B2c})$$

$$2\text{Re}(F^{(a)} \Delta F^{(b)\dagger}) = -\text{Re} \left\{ \sqrt{\frac{8}{\pi}} f^{\gamma^* N \rightarrow VN}(\mathbf{l}) S_d^{s,mm'}(\mathbf{l}_\perp/2, -l_-/2) \right.$$

$$\times \int \frac{d^2 k_\perp}{(2\pi)^2} f^{\gamma^* N \rightarrow VN}(\mathbf{l}_\perp/2 - \mathbf{k}_\perp)^\dagger f^{VN \rightarrow VN}(\mathbf{l}_\perp/2 + \mathbf{k}_\perp)^\dagger \Delta S_d^{s,mm'}(\mathbf{k}_\perp, -\Delta_V) \Big\}, \quad (\text{B2d})$$

$$2\text{Re}(\tilde{F}^{(b)} \Delta F^{(b)\dagger}) = -\text{Im} \left\{ \frac{1}{\sqrt{2\pi}} \int \frac{d^2 k_\perp}{(2\pi)^2} \frac{d^2 k'_\perp}{(2\pi)^2} f^{\gamma^* N \rightarrow VN}(\mathbf{l}_\perp/2 - \mathbf{k}_\perp) \right. \\ \times f^{VN \rightarrow VN}(\mathbf{l}_\perp/2 + \mathbf{k}_\perp) f^{\gamma^* N \rightarrow VN}(\mathbf{l}_\perp/2 - \mathbf{k}'_\perp)^\dagger f^{VN \rightarrow VN}(\mathbf{l}_\perp/2 + \mathbf{k}'_\perp)^\dagger \\ \left. \times S_d^{s,mm'}(\mathbf{k}_\perp, -\Delta_V) \Delta S_d^{s,mm'}(\mathbf{k}'_\perp, -\Delta_V) \right\}, \quad (\text{B2e})$$

$$\Delta F^{(b)} \Delta F^{(b)\dagger} = \frac{1}{2\pi} \int \frac{d^2 k_\perp}{(2\pi)^2} \frac{d^2 k'_\perp}{(2\pi)^2} f^{\gamma^* N \rightarrow VN}(\mathbf{l}_\perp/2 - \mathbf{k}_\perp) f^{VN \rightarrow VN}(\mathbf{l}_\perp/2 + \mathbf{k}_\perp) \\ \times f^{\gamma^* N \rightarrow VN}(\mathbf{l}_\perp/2 - \mathbf{k}'_\perp)^\dagger f^{VN \rightarrow VN}(\mathbf{l}_\perp/2 + \mathbf{k}'_\perp)^\dagger \\ \times \Delta S_d^{s,mm'}(\mathbf{k}_\perp, -\Delta_V) \Delta S_d^{s,mm'}(\mathbf{k}'_\perp, -\Delta_V). \quad (\text{B2f})$$

APPENDIX C: DEUTERIUM FORM FACTOR AND DENSITY MATRIX

In coherent vector meson production processes the form factor which enters in Eqs.(2,12) is the elastic deuteron form factor. It can be split into a monopole and a quadrupole term (see e.g. Ref. [33]):

$$S_d^{s,mm'}(\mathbf{l}) = \chi_d^{m\dagger} \left(F_C(l) - F_Q(l) \sqrt{\frac{1}{8}} \hat{S}(\mathbf{l}) \right) \chi_d^{m'}. \quad (\text{C1})$$

Here χ_d^m is the deuteron spinor, $\hat{S}(\mathbf{l}) = 3(\boldsymbol{\sigma}_p \cdot \mathbf{l})(\boldsymbol{\sigma}_n \cdot \mathbf{l})/l^2 - \boldsymbol{\sigma}_p \cdot \boldsymbol{\sigma}_n$ the tensor operator and $l = |\mathbf{l}|$. The index s specifies the spin quantization axis, while $m, m' = 0, +, -$ label the spin projection of the deuteron before and after the interaction, respectively. The monopole and quadrupole form factor can be expressed in terms of u and w , the radial S - and D -state wave functions of the deuteron:

$$F_C(l) = \int_0^\infty dr \left[u^2(r) + w^2(r) \right] j_0(lr), \\ F_Q(l) = \int_0^\infty dr \left[u(r) - \frac{1}{\sqrt{8}} w(r) \right] 2w(r) j_2(lr). \quad (\text{C2})$$

If the spin polarization of the final state deuteron is not observed the coherent scattering amplitudes can be written in terms of the density matrix [34]:

$$\rho^{s,m}(\mathbf{l}_1, \mathbf{l}_2) = \sum_{m'} S_d^{s,mm'}(\mathbf{l}_1) S_d^{s,mm'}(\mathbf{l}_2)^\dagger = F_C(l_1) F_C(l_2) \\ + \frac{1}{\sqrt{2}} \left\{ \left[\frac{3|\mathbf{l}_2 \cdot \boldsymbol{\epsilon}_s^m|^2}{l_2^2} - 1 \right] F_C(l_1) F_Q(l_2) + \left[\frac{3|\mathbf{l}_1 \cdot \boldsymbol{\epsilon}_s^m|^2}{l_1^2} - 1 \right] F_C(l_2) F_Q(l_1) \right. \\ \left. + \left[9 \frac{(\mathbf{l}_1 \cdot \boldsymbol{\epsilon}_s^m)(\mathbf{l}_1 \cdot \boldsymbol{\epsilon}_s^m)^* \mathbf{l}_1 \cdot \mathbf{l}_2}{l_1^2 l_2^2} - \frac{3|\mathbf{l}_1 \cdot \boldsymbol{\epsilon}_s^m|^2}{l_1^2} - \frac{3|\mathbf{l}_2 \cdot \boldsymbol{\epsilon}_s^m|^2}{l_2^2} + 1 \right] \frac{F_Q(l_1) F_Q(l_2)}{2} \right\}. \quad (\text{C3})$$

Here $\boldsymbol{\epsilon}_s^m$ is the polarization vector of the target deuteron. For spin quantization parallel to the z axis we have:

$$\boldsymbol{\epsilon}^+ = \frac{-1}{\sqrt{2}} \begin{pmatrix} 1 \\ i \\ 0 \end{pmatrix}, \quad \boldsymbol{\epsilon}^- = \frac{1}{\sqrt{2}} \begin{pmatrix} 1 \\ -i \\ 0 \end{pmatrix}, \quad \boldsymbol{\epsilon}^0 = \begin{pmatrix} 0 \\ 0 \\ 1 \end{pmatrix}. \quad (\text{C4})$$

Note that for practical purposes the representation of the spin density matrix in (C3) in terms of the polarization vector $\boldsymbol{\epsilon}_s^m$ is very useful since it is applicable for any choice of the spin quantization axis after rotating the polarization vectors appropriately.

REFERENCES

- [1] L.L. Frankfurt, G.A. Miller and M.I. Strikman, *Ann. Rev. Nucl. Part. Sci.* **45** (1994) 501; P. Jain, B. Pire and J.P. Ralston, *Phys. Rep.* **271** (1995) 133.
- [2] T.H. Bauer, R.D. Spital, D.R. Yennie and F.M. Pipkin, *Rev. Mod. Phys.* **50** (1978) 261.
- [3] S.J. Brodsky, L.L. Frankfurt, J.F. Gunion, A.H. Mueller and M.I. Strikman, *Phys. Rev.* **D50** (1994) 3134.
- [4] H. Cheng and T. T. Wu *Phys. Rev.* **183** 1324 (1970).
- [5] J. B. Kogut, *Phys. Rev.* **D5**, 1152 (1972).
- [6] L.L. Frankfurt, W. Koepf and M.I. Strikman, *Phys. Rev.* **D54**, (1996) 3194.
- [7] V.N. Gribov, B.L. Ioffe and I.Ya. Pomeranchuk, *Soviet Journal of Nucl. Phys.* **2** (1966) 549.
- [8] V.N. Gribov, *JETP* **30** (1970) 709.
- [9] C. Llewellyn-Smith, *Phys.Rev.* **D4** (1971) 2392.
- [10] B. L. Ioffe, *Phys. Lett.* **30** (1968) 123.
- [11] M. Arneodo, *Phys. Rep.* **240** (1994) 301.
- [12] R.D. Spital and D.R. Yennie, *Nucl. Phys.* **106** (1976) 269 .
- [13] D. R. Yennie, in *Hadronic Interactions of Electrons and Photons*, edited by J. Cummings and D. Osborn, **321** (1971).
- [14] J. Hüfner, B. Kopeliovich and J. Nemchik, *Phys. Lett.* **383** (1996) 362.
- [15] V. Franco and R.J. Glauber, *Phys. Rev.* **142** (1966) 1195.
- [16] L. Bertocchi and A. Capella, *Il Nuovo Cimento* **A51** (1967) 369.
- [17] M. Arneodo et al., *Nucl. Phys.* **B429** (1994) 503; M. Derrick et al., *Phys. Lett.* **B356** (1995) 601; S. Aid et al., *Nucl. Phys.* **B468** (1996) 3.
- [18] V. Franco and R.J. Glauber, *Phys. Rev. Lett.* **22** (1969) 370
- [19] J.D. Bjorken, *Phys. Rev.* **148** (1966) 1467.
- [20] A.H. Mueller, *Phys. Rev.* **D2** (1970) 2963; *ibid.* **D4** (1971) 150.
- [21] H. Abramowicz, L.L. Frankfurt and M.I. Strikman, DESY-95047, 1995.
- [22] L.L. Frankfurt, V. Guzey, W. Koepf, M. Sargsyan and M.I. Strikman, *In Proceedings of the Workshop "Future Physics at HERA"*, 1996, Vol.II, p.946
- [23] J. Collins, L.L. Frankfurt and M.I. Strikman, CERN-TH/96-314, PSU/TH/168, hep-ph/9611433, 1996.
- [24] H. Fraas and D. Schildknecht, *Nucl. Phys.* **B14** (1969) 543.
- [25] D.G. Cassel, L.A. Ahrens et al., *Phys. Rev.* **D24** (1981) 2787.
- [26] I.D. Overman, PhD thesis, SLAC-140, UC-34, 1971.
- [27] R.L. Anderson et al., *Phys. Rev.* **D4** (1971) 3245.
- [28] W. Brooks et al., LOI-004, CEBAF, 1995.
- [29] L.L. Frankfurt, et al., *Proceedings of the Workshop on Future Physics at HERA (DESY), Hamburg, 1996*; L.L. Frankfurt, et al., *Proceedings of the 2nd ELFE Workshop, St. Malo, 1996*.
- [30] M. Lacombe, B. Loiseau, J.M. Richard and R.V. Mau, *Phys. Rev.* **C21** (1980) 861.
- [31] H. Cheng and T.T. Wu, *Expanding Protons: Scattering at High Energies* (MIT Press, Cambridge, 1987).
- [32] L.L. Frankfurt and M.I. Strikman, *Phys. Rep.* **76**, (1981) 215.
- [33] G.E. Brown and A.D. Jackson, *The Nucleon-Nucleon Interaction* (North-Holland, Amsterdam, 1976).

- [34] A.B. Akhiezer and V.M. Berestecky, *Quantum Electrodynamics* (Interscience, New York, 1965).

FIGURES

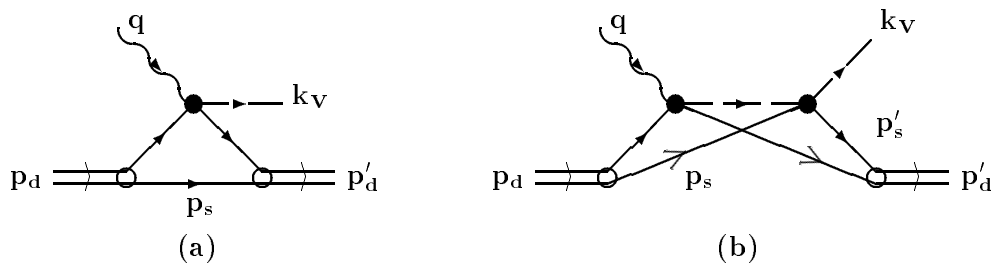


Figure 1

Single scattering (a) and double scattering contribution (b) to exclusive vector meson production in photon-deuteron collisions.

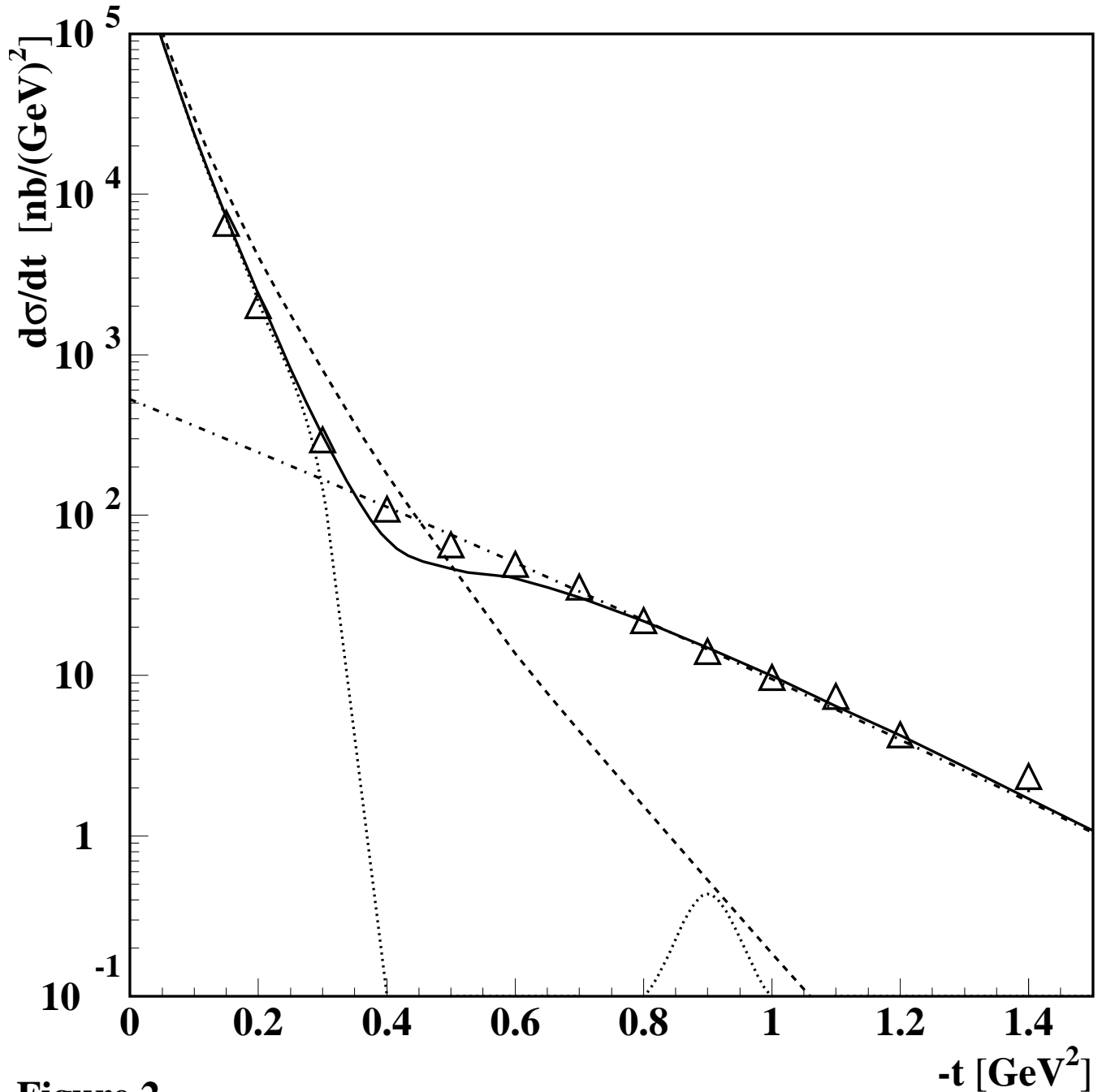


Figure 2

The cross section $d\sigma_{\gamma d \rightarrow \rho d}/dt$ for photoproduction of ρ -mesons from unpolarized deuterium. The full curve shows the result of our calculation within vector meson dominance. The dashed, dotted and dash-dotted lines account for the Born, interference, and double scattering contribution, respectively. The experimental data are from Ref. [26,27] taken at a photon energy $\nu = 12 \text{ GeV}$.

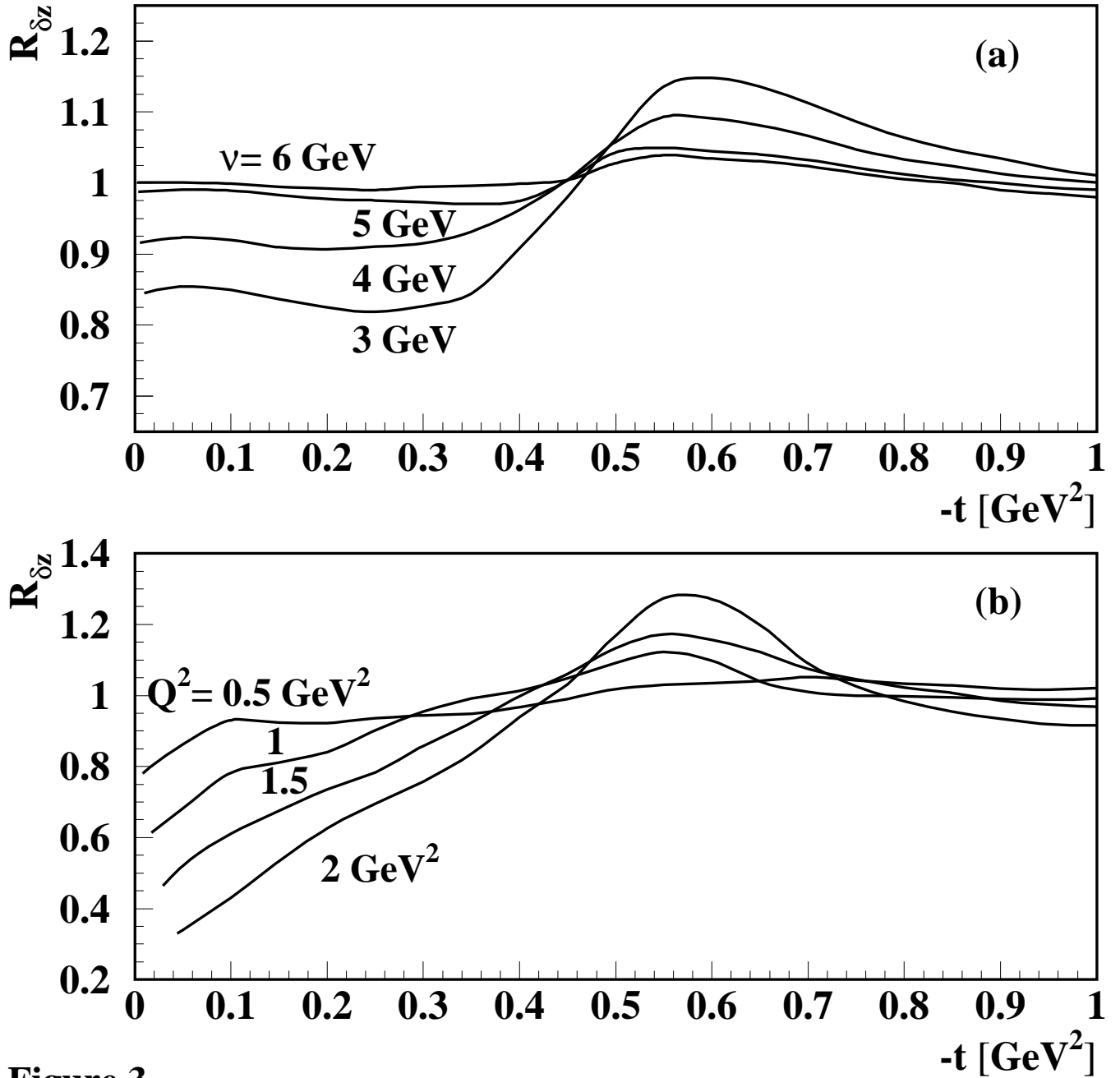


Figure 3

The cross section ratio R_{δ_z} from (36) plotted against t for photoproduction (a) and lepton production (b) at $\nu = 6$ GeV.

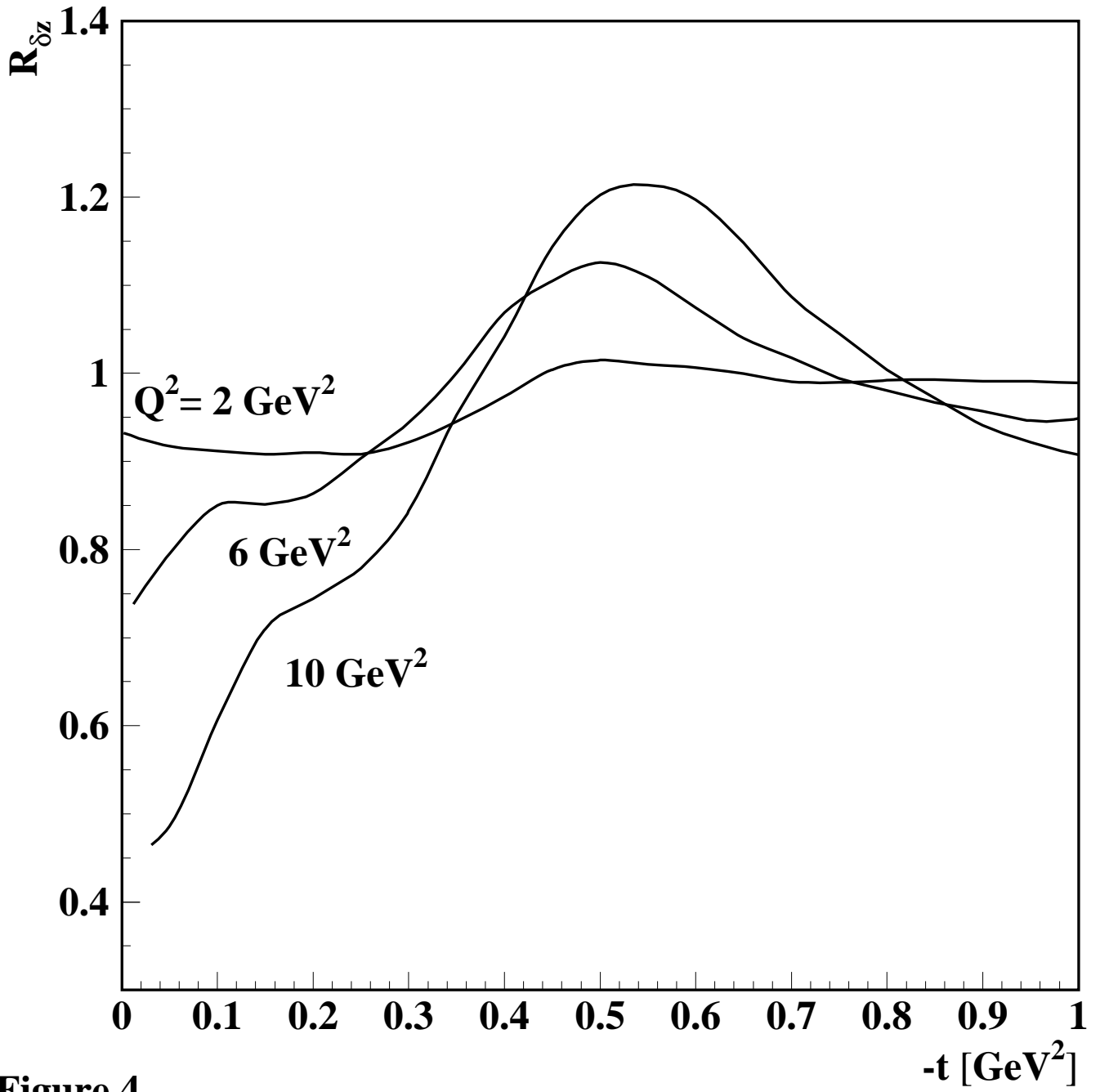


Figure 4

The cross section ratio R_{δ_z} from (36) for $\nu = 30 \text{ GeV}$ and various values of Q^2 .

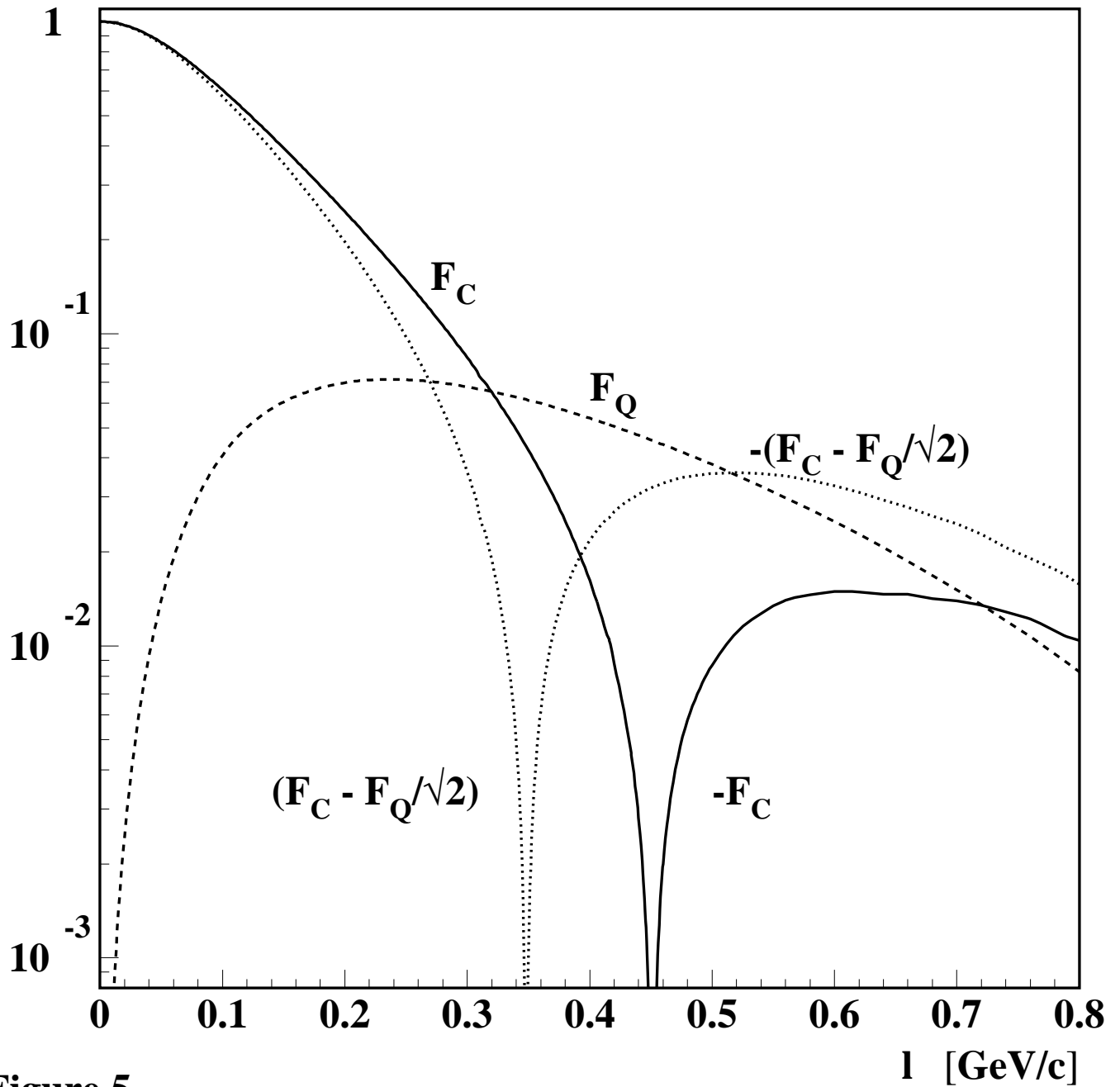


Figure 5

The momentum dependence of the deuteron form factor (C2) for the Paris potential [30]. The charge, F_C , and quadrupole form factor, F_Q , are shown as well as the combination $F_C - F_Q/\sqrt{2}$.

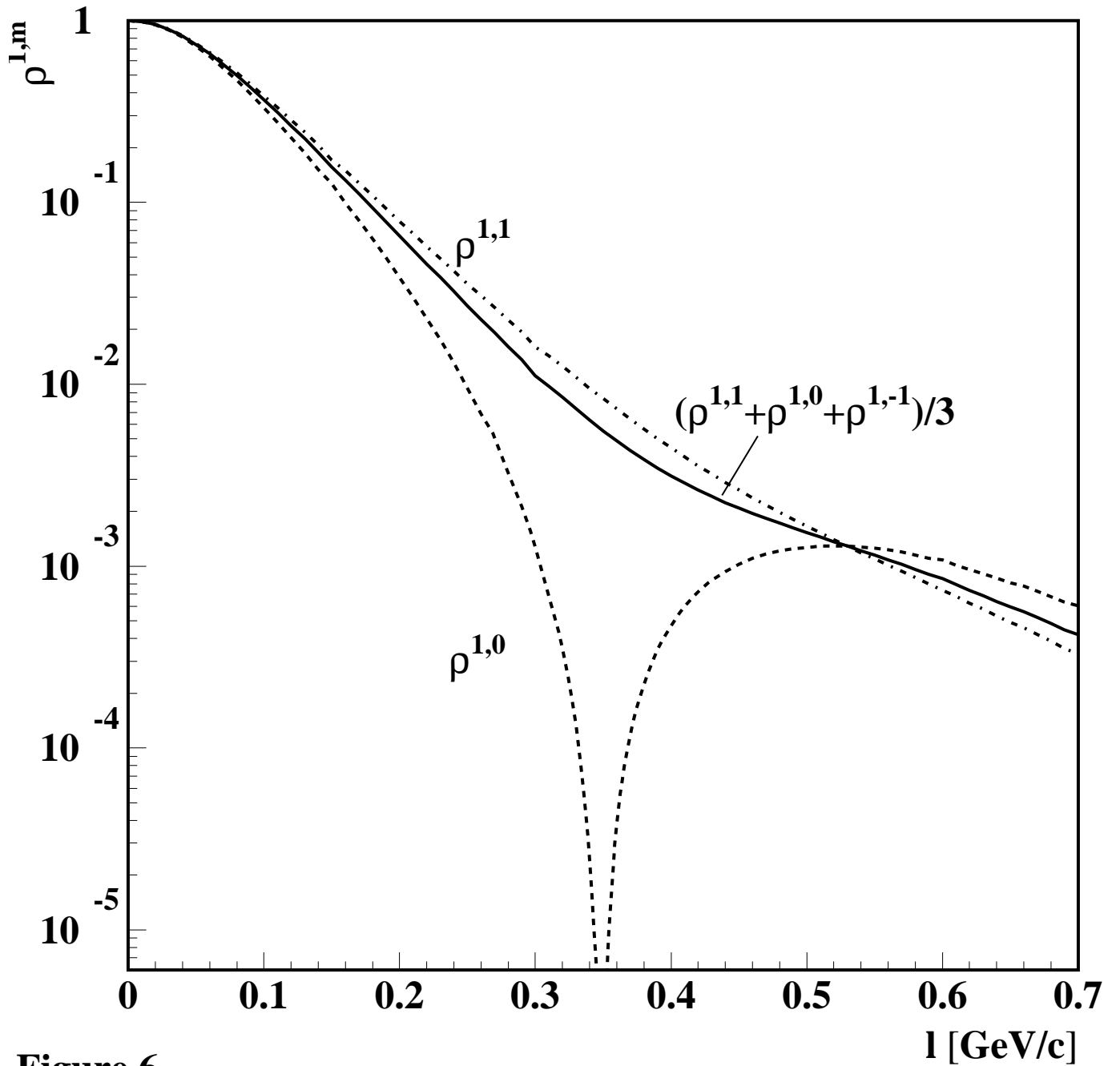


Figure 6

The deuteron density matrix $\rho^{1,m}$ from (37) for a spin quantization axis parallel to the photon momentum \mathbf{q} . The dashed and dash-dotted lines correspond to spin projections $m = 0$ and $m = 1$, respectively. The density matrix for an unpolarized deuteron is shown by the solid curve.

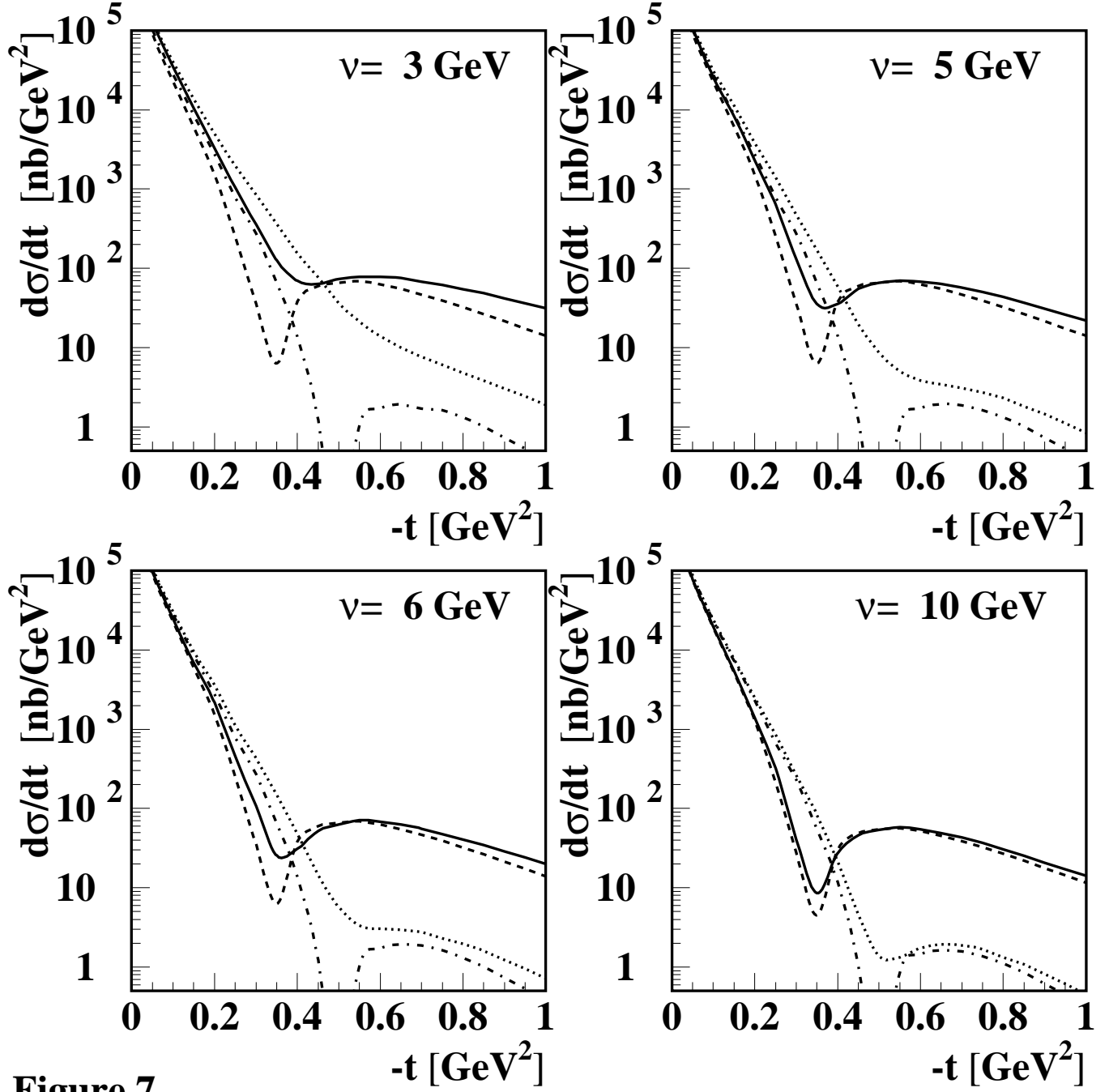


Figure 7

The differential cross section $d\sigma_{\gamma d \rightarrow \rho d}^{10}/dt$ for the photoproduction of ρ -mesons from polarized deuterium for different photon energies. The target polarization is fixed at $m = 0$ with respect to the photon momentum ($s = 1$). The solid curves show the complete vector meson dominance result. The dotted curves represent the Born contribution only. The dashed and dash-dotted curves show the full and the Born cross section for infinite longitudinal interaction lengths $\delta_z^{(a)}, \delta_z^{(b)} \rightarrow \infty$.

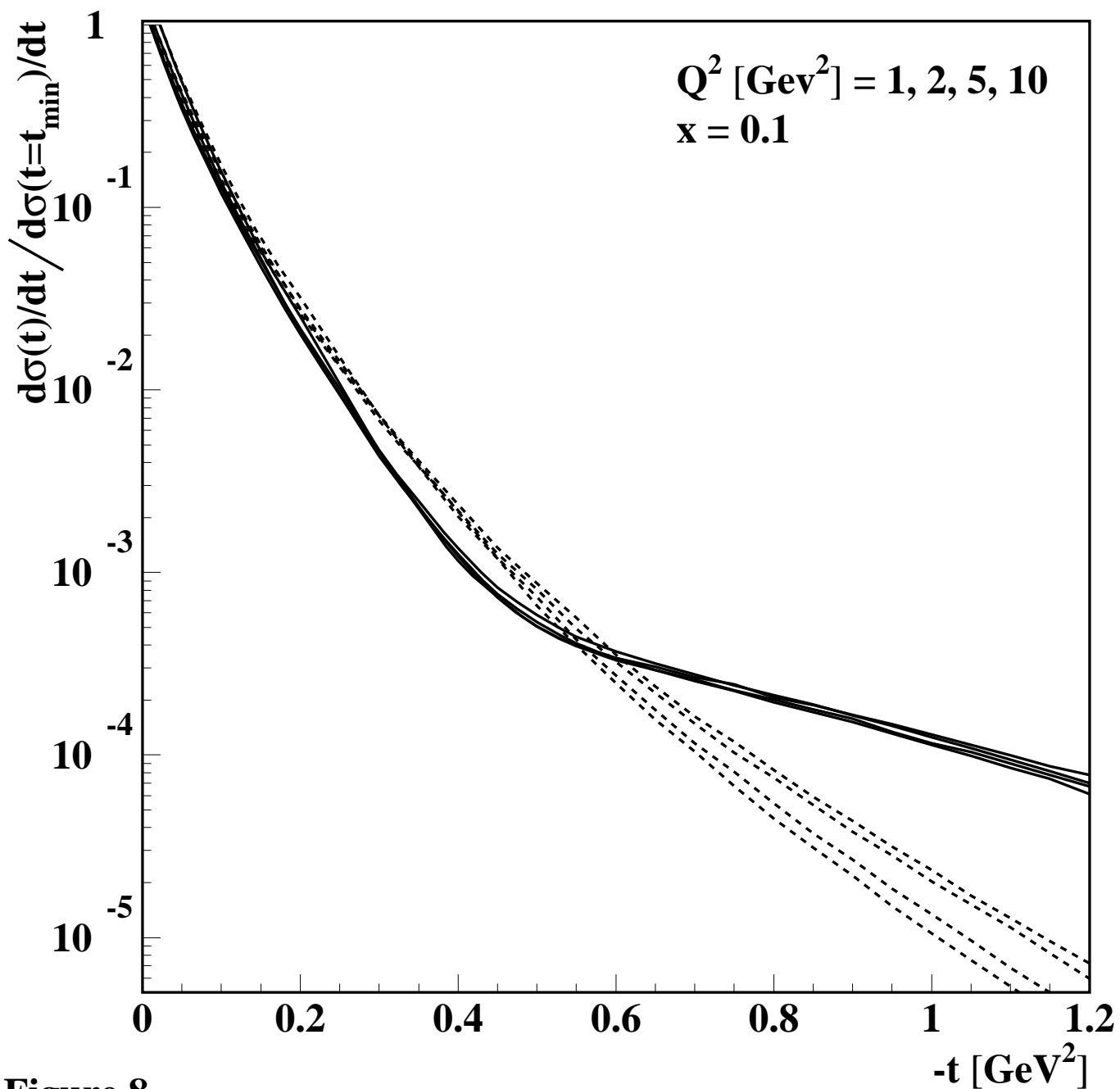
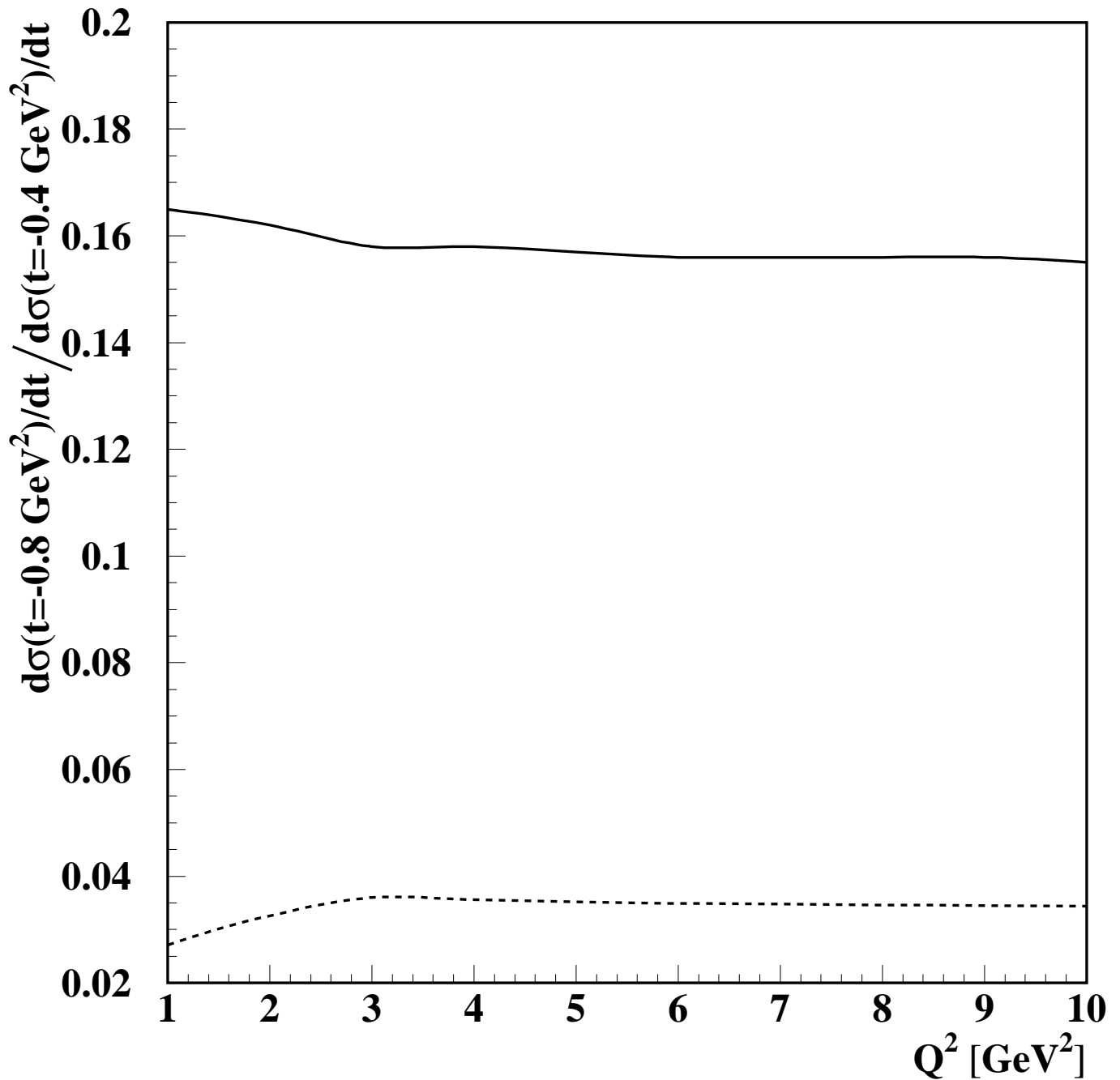


Figure 8

The cross section ratio R from (41) for $x = 0.1$ and various values of Q^2 . The solid lines represent the complete result of vector meson dominance. The dashed curves show the Born contribution.



The Q^2 -dependence of the ratio $R(t = -0.8 \text{ GeV}^2)/R(t = -0.4 \text{ GeV}^2)$ from (41). The solid line represents the complete vector meson dominance calculation. The dashed curve accounts for the Born contribution only.

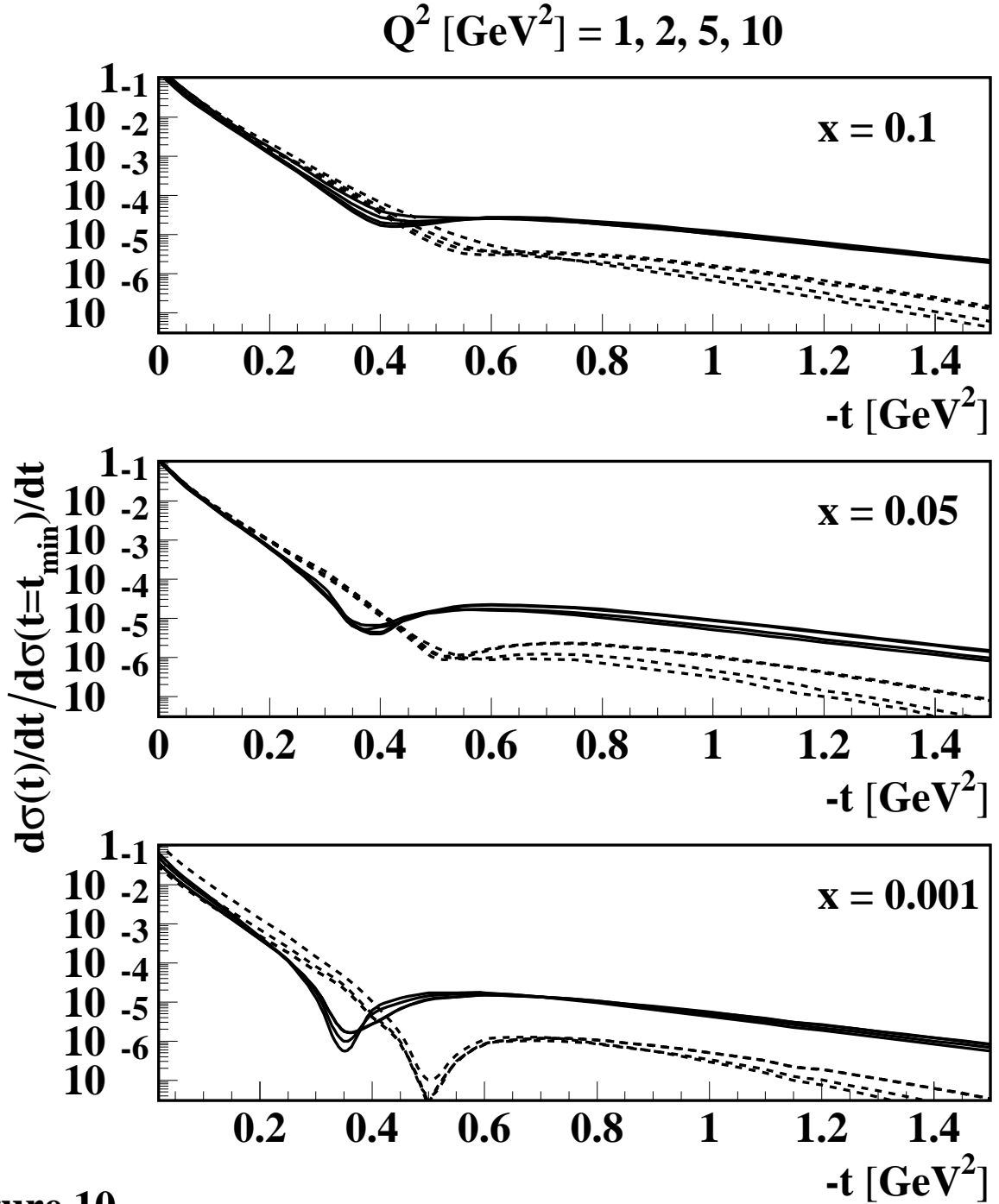


Figure 10

The cross section ratio $R^{1,0}$ from (42) for $x = 0.1, 0.05, 0.01$, and various values of Q^2 . The solid lines represent the complete vector meson dominance calculation. The dashed curves show the Born contribution.

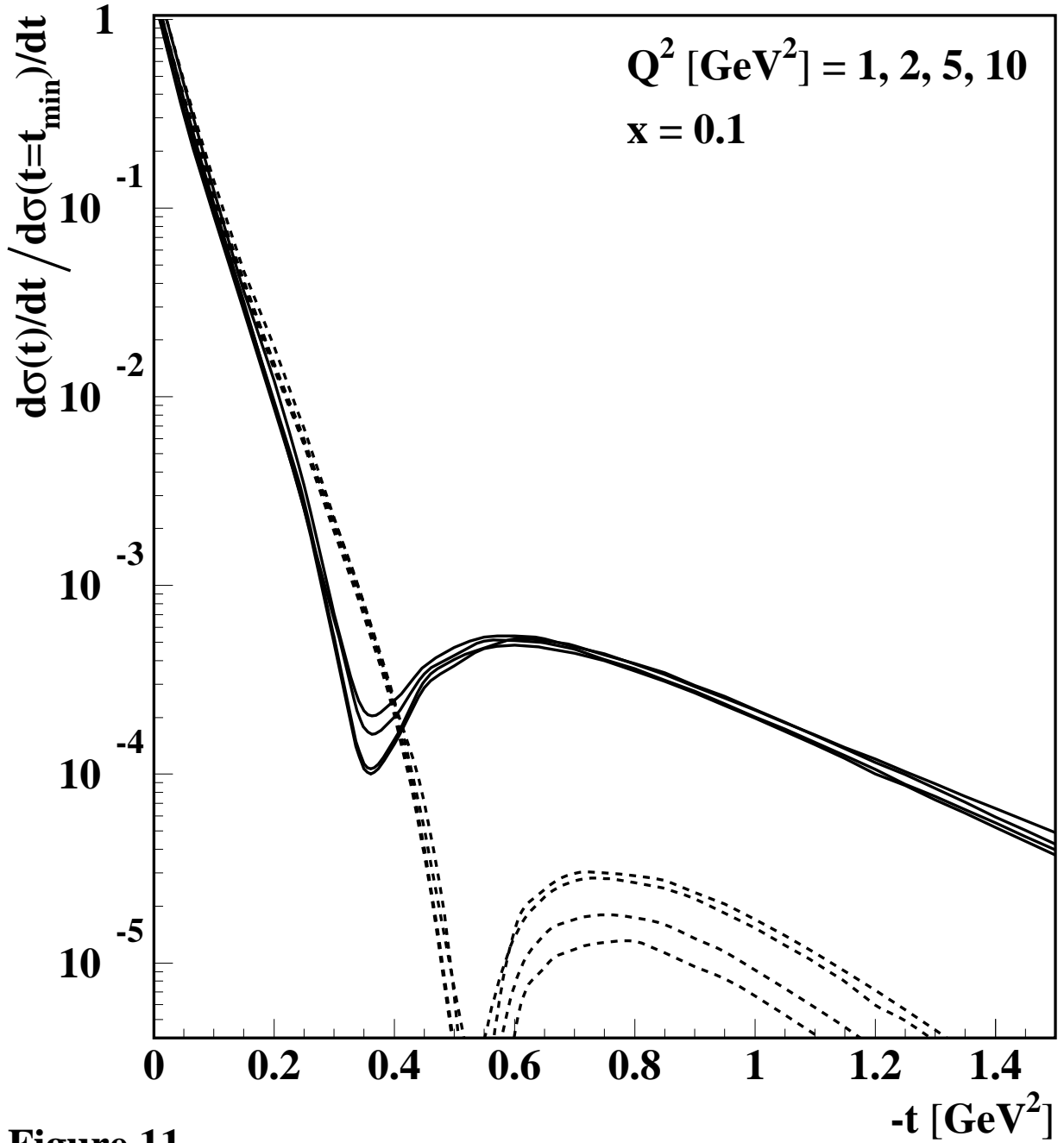


Figure 11

The cross section ratio $R^{2,0}$ (43) for $x = 0.1$ and various values of Q^2 . The solid lines represent the complete vector meson dominance calculation. The dashed curves show the Born contribution.

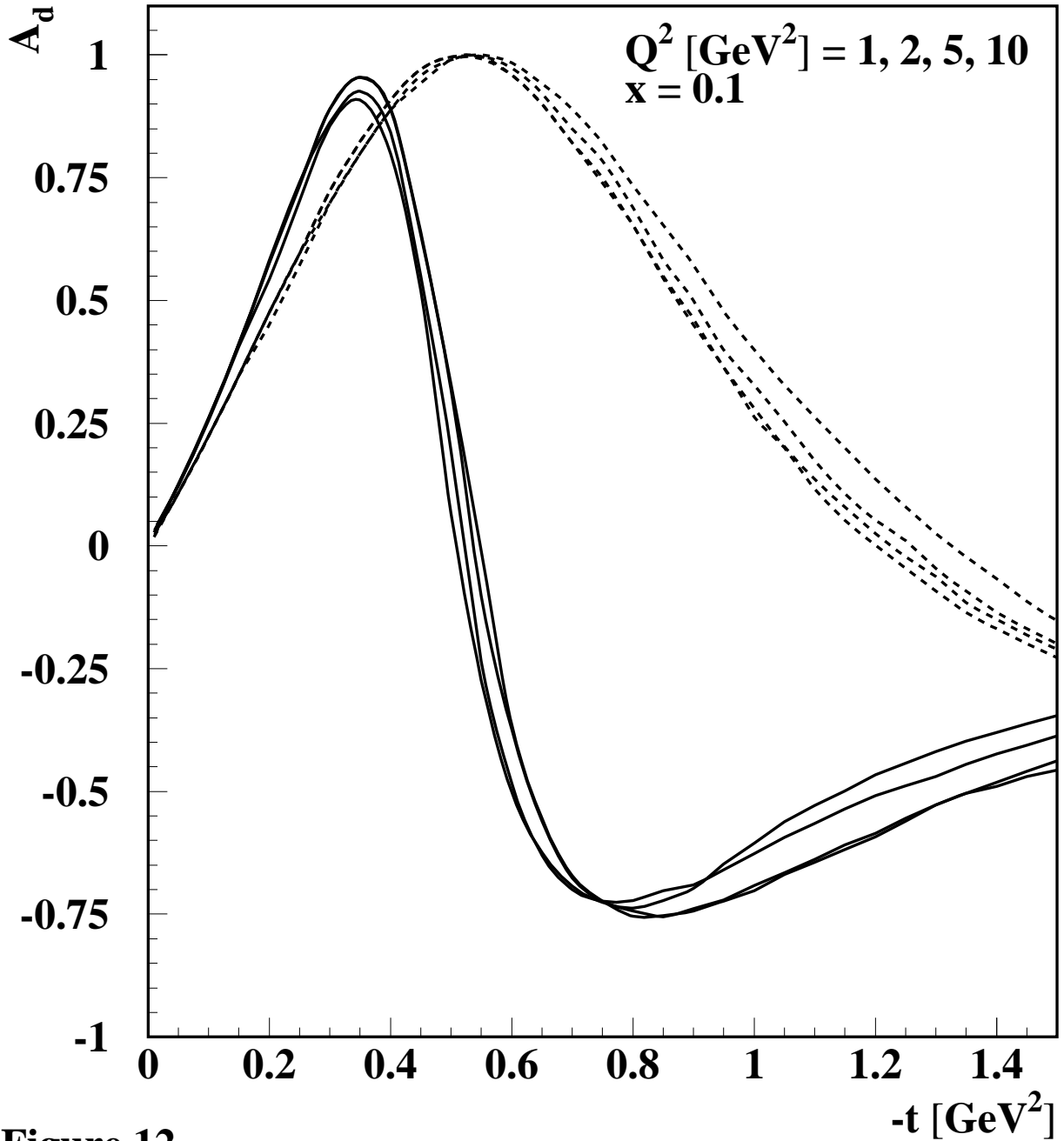


Figure 12

The tensor polarization asymmetry A_d from (44) for $x = 0.1$ and various values of Q^2 . The spin quantization axis is chosen parallel to $\boldsymbol{\kappa} \sim \mathbf{q} \times \mathbf{l}$. The solid lines represent the complete vector meson dominance calculation. The dashed curves show the Born contribution.